INTERNATIONAL JOURNAL FOR NUMERICAL METHODS IN ENGINEERING
*Int. J. Numer. Meth. Engng.* **47**, 395–418 (2000)

# A variational principle for the formulation of partitioned structural systems

K. C. Park and Carlos A. Felippa *

*Department of Aerospace Engineering Sciences and Center for Aerospace Structures, University of Colorado at Boulder, Boulder, CO 80309-0429, U.S.A.*

SUMMARY

A continuum-based variational principle is presented for the formulation of the discrete governing equations of partitioned structural systems. This application includes coupled substructures as well as subdomains obtained by mesh decomposition. The present variational principle is derived by a series of modifications of a hybrid functional originally proposed by Atluri for finite element development. The interface is treated by a displacement frame and a localized version of the method of Lagrange multipliers. Interior displacements are decomposed into rigid-body and deformational components to handle floating subdomains. Both static and dynamic versions are considered. An important application of the present principle is the treatment of nonmatching meshes that arise from various sources such as separate discretization of substructures, independent mesh refinement, and global–local analysis. The present principle is compared with that of a globalized version of the multiplier method. Copyright © 2000 John Wiley & Sons, Ltd.

KEY WORDS: variational principles; hybrid principles; interface potentials; partitioned analysis; multilevel analysis; Lagrange multipliers; finite element methods; non-matching meshes; structural dynamics; parallel computation

## 1. INTRODUCTION

The decomposition of discrete models of mechanical systems has received increased attention in recent years. Research into that topic has been driven by the analysis of coupled systems, the solution of inverse problems and the use of massively parallel computers. This paper studies a specific class of decompositions: the partitioned analysis of mechanical systems.

The term *partitioning* identifies the process of *spatial* separation of a discrete mechanical model into interacting components generically called *partitions*. The decomposition may be driven by physical, functional, or computational considerations. For example, the structure of a complete airplane can be decomposed into substructures such as wings and fuselage according to *function*. Substructures can be further decomposed into submeshes or subdomains to accommodate parallel *computing* requirements. Going the other way, if that flexible airplane is part of a flight simulation, a top-level partition driven by *physics* consists of fluid and structure (and perhaps

* Correspondence to: Carlos A. Felippa, Department of Aerospace Engineering Sciences, University of Colorado at Boulder, Campus Box 429, Boulder, CO 80309-0429, U.S.A. E-mail: carlos.felippa@colorado.edu

Contract/grant sponsor: National Science Foundation; contract/grant number: ECS-9725504
Contract/grant sponsor: Sandia National Laboratories; contract/grant numbers: AS-5666 and AS-9991

CCC 0029-5981/2000/020395–24$17.50 *Received 8 March 1999*

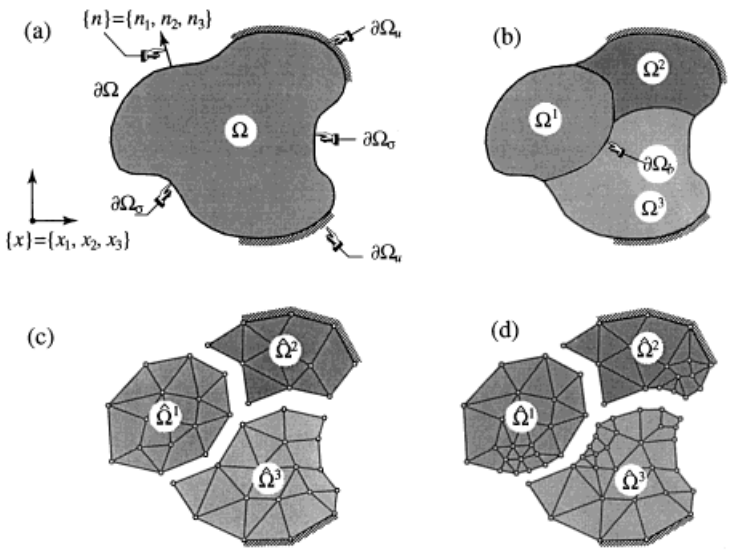


Figure 1. (a) A domain $\Omega$ with boundary $\partial\Omega = \partial\Omega_\sigma \cup \partial\Omega_u$; (b); partition into three subdomains: $\Omega^1$, $\Omega^2$ and $\Omega^3$ by cutting it through interface $\partial\Omega_b$. Two FEM discretizations of (b); (c) matching submeshes; (d) non-matching submeshes. Superposed hats distinguish discrete versions

control and propulsion) models. This kind of multilevel partition hierarchy, viz. coupled system, structure, substructure and subdomain, is typical of present practice in modelling and computational technology.

Partitioned analysis stipulates that the discretization of individual components through standard methods (such as finite elements, finite differences or boundary elements) is well on hand. The problem is thereby reduced to modelling the *interaction* of those components. For simple decompositions, as in a mechanical mesh collocated to another, this can be handled by well-known primal or dual techniques, such as degree of freedom matching or standard Lagrange multipliers.

Complications may be introduced into the picture, however, by several factors. Physically heterogeneous models may be the product of different discretization techniques, as exemplified by a pressure-based fluid BEM mesh coupled to a displacement-based FEM structural mesh. Nodes on both sides of an interface may be non-matching, sliding or moving; the latter being typical of contact and impact problems. Finally, multilevel decompositions bring combinatorial complexity.

A source of non-matching meshes is illustrated in Figure 1. The domain $\Omega$ of Figure 1(a) is divided into three subdomains by an interface $\partial\Omega_b$ as depicted in Figure 1(b). Figure 1(c) shows a FEM discretization with matching meshes. This typically results by discretizing the whole domain first, followed by mesh decomposition. If subdomain meshes are subsequently refined without consideration of interconnections, non-matching meshes may result as pictured in Figure 1(d). Note that if the interface segments are curved as in this example, the discrete interfaces do not generally overlap in space and their normals may be misaligned.

To handle such a wide variety of scenarios it is useful to develop a general continuum variational framework, from which specific partitioned formulations and solution algorithms can be developed and tested. The situation is analogous to the transition that took place in the development of the finite element method from matrix structural analysis to continuum-based variational principles,

 

which are by now well established. These 'coupling principles' should be powerful enough to model physically heterogeneous interfaces, handle non-matched discrete nodal distributions, and guide the rational choice of admissible discretization function spaces along the partition boundaries.

The present paper addresses the construction of such principles for structural mechanics models. The main novel features are: (i) the use of separately varied partition-frame displacements and Lagrange multipliers to link arbitrarily connected meshes of mechanical finite elements, and (ii) the explicit separation of rigid-body and deformational motions so that the solvability conditions for floating partitions are automatically provided as part of the formulation.

## 2. VARIATIONAL PRINCIPLES AND LAGRANGE MULTIPLIERS

There exist a rich body of literature on the variational principles in structural mechanics. Survey articles and book chapters oriented to such applications may be found in [1–11].

Most of these principles were developed with finite element models in mind. In particular, developments of hybrid and mixed principles since the mid-1960s, pioneered by Pian [12] and Herrmann [13], were largely driven by the goal of relaxing displacement continuity requirements so as to formulate better performing elements. Those principles introduce additional independent variables which, as pointed out by Fraeijs de Veubeke in several important articles [2, 14, 15] may be viewed as an application of the method of Lagrange multiplier fields. Those fields are adjoined through standard techniques such as Friedrichs' dislocation potentials [16] or Legendre transforms [17]. In hybrid principles the multipliers may be physically interpreted as internal fields such as stresses, pressures, tractions or strains. Upon discretization the associated variables are eliminated at the element level to produce elements with the standard external displacement degrees of freedom.

It is recalled that Lagrange's original motivation for what he called the 'method of indeterminate coefficients' was to derive the equilibrium equations of a system of constrained rigid bodies, or 'particles' in Newtonian mechanics parlance. To this end, Lagrange treated the problem 'as if all bodies are entirely free' and formulated the virtual work by summing up the contributions of 'entirely free' individual bodies. He then identified the 'equations of condition' (in modern terminology, the constraint equations) among the kinematic differential variables. Once identified, each constraint equation was multiplied by an indeterminate coefficient and added to the virtual work of the free bodies to yield the total virtual work of the system. He states: 'the sum of all the terms which are multiplied by the same differential (same variation in modern usage) are equated to zero, which will give as many particular solutions as there are differentials. … These equations, being then rid of the indeterminate coefficients by elimination, will provide all of the conditions necessary for equilibrium'. See [18–20]. Hence the notion of eventual elimination of multipliers has strong historical roots.

The partitioning scheme considered here *retains* Lagrange multipliers on interfaces rather than eliminating them. It represents a continuum generalization of the Localized Lagrange Multiplier (LLM) method, presented by Park and Felippa [21] for discrete mechanical systems whose interface freedoms match. For matching meshes one advantage of the LLM method over the classical multiplier method is the treatment of the so-called cross points, namely nodes whose freedoms are shared by more than two submeshes. The LLM method yields a unique set of constraint conditions. That appealing simplicity breaks down for non-matching meshes. To handle those complications it is convenient to move to a continuum level framework, and treat multipliers as interface fields to

 

be appropriately interpolated. Those interpolation functions cannot be arbitrarily chosen, but must satisfy Fraeijs de Veubeke's limitation principle [2]. The LLM for matched meshes is recovered as a particular case, in which the interface multipliers are interpolated by node-collocated delta functions.

When multipliers are retained as interface connectors the 'floating partition' problem arises. In the standard displacement formulation of finite elements the rigid-body modes (RBM) are implicitly embodied in the strain–displacement equations. Upon assembly and application of support conditions the discrete stiffness equations are rid of RBMs (except in special problems, such as free-free dynamics). In multiplier-connected systems the RBMs of each partition must be explicitly identified and be in self-equilibrium under rigid-body motions. This self-equilibrium condition was apparently first stated by Fraeijs de Veubeke [22] as providing the fundamental solvability conditions for disconnected elements. It has played a pivotal role in the development of the Finite Element Tearing and Interconnecting (FETI) method developed by Farhat, Roux and coworkers [23–26] for parallel computation of structural mechanics problems. These precursors to the present formulation are discussed in Section 6.

## 3. CONTINUUM VARIATIONAL FORMULATION

In a 1975 article, Atluri [6] presented two hybrid functionals, labeled HWM1 and HWM2 (for 'Hu–Washizu Modified'), which collectively extend the Hu–Washizu (HW) principle to accommodate internal interfaces. The five-field functional HMW1 extends HW with the interface discontinuity term proposed by Prager [27], which links interface displacements through a single Lagrange multiplier field. The six-field functional HWM2 includes independently varied boundary displacements weakly linked to interior displacements by subdomain-localized Lagrange multipliers fields. This approach is relevant to the present development.

### *3.1. The HMW2 functional*

Key ingredients of HWM2 are illustrated in Figures 1 and 2. The elastic body of Figure 1(a) occupies domain $\Omega$, referred to a Cartesian system $x_i$. The boundary $\partial\Omega$ has exterior normal $n_i$. The domain is partitioned into three subdomains $\Omega_1$, $\Omega_2$ and $\Omega_3$ as depicted in Figure 2(a). An internal boundary $\partial\Omega_{\mathrm{b}}$ called a *partition frame*, is placed as shown in Figure 2(b). The displacements of $\partial\Omega_{\mathrm{b}}$ are to be varied independently from those of the subdomains. The partition frame is 'glued' to the adjacent subdomains by Lagrange multiplier fields $\lambda_{\mathrm{l}}$. These multipliers are said to be *localized* because they are associated with subdomains.

The interior fields of subdomain $\Omega^m$, considered as an isolated entity, are: displacements $u_i^m$, strain $\varepsilon_{ij}^m$, stress $\sigma_{ij}^m$ and prescribed body force $\bar{f}_i^m$. Its boundary $\partial\Omega^m$ can be generally decomposed into $\partial\Omega_u^m, \partial\Omega_\sigma^m$ and $\partial\Omega_{\mathrm{b}}^m$. $\partial\Omega_u^m$ and $\partial\Omega_\sigma^m$ are portions of $\partial\Omega^m$ where displacements $\bar{u}_i$ and tractions $\bar{t}_i$, respectively, are prescribed. $\partial\Omega_{\mathrm{b}}^m$ is the interface with other subdomains, over which the Lagrange multiplier field $\lambda_{\mathrm{l}i}^m$ has the role of surface traction. Subdomain linking is done through the displacement $u_{\mathrm{b}i}$ of the partition frame $\partial\Omega_{\mathrm{b}}$. The strain energy density and symmetric displacement gradients are denoted by

$$\mathscr{U}(\varepsilon_{ij}) = \tfrac{1}{2} E_{ijkl}\, \varepsilon_{ij}\, \varepsilon_{kl}, \quad u_{(i,j)} = \tfrac{1}{2}(u_{i,j} + u_{j,i}) \tag{1}$$

 

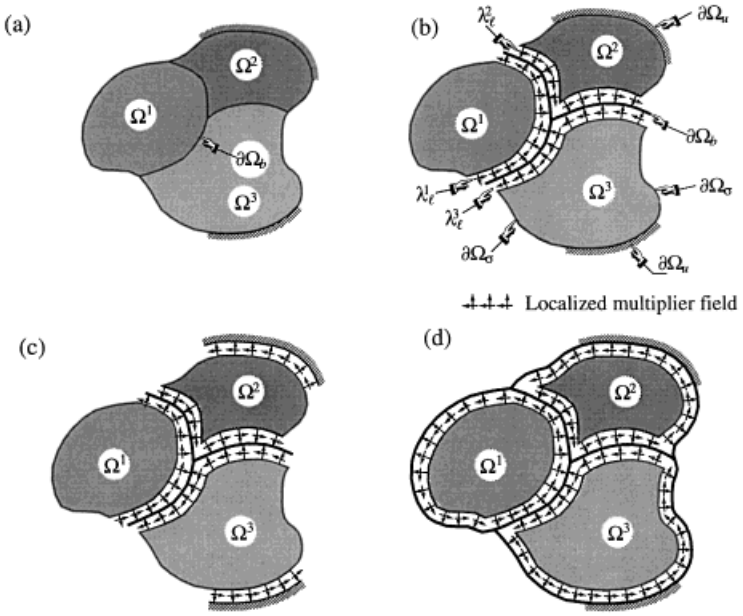


Figure 2. Interface treatment used in constructing several functionals. (a) The domain of Figure 1(a) divided into three subdomain partitions; (b) Functional $\Pi_{\mathrm{HWM2}}$: linkup by localized Lagrange multipliers and partition-frame displacements; (c) Functional $\Pi_{\mathrm{PEM2}}$: the multiplier fields are extended to include prescribed-displacement portions $\partial\Omega_u$; (d) Functional $\Pi_{\mathrm{UFF}}$: the multiplier fields are extended to cover all boundaries, whether internal or external

respectively, in which $E_{ijkl}$ are the elastic moduli, commas denote partial derivatives, and the summation convention is in effect. With these ingredients in place, the HWM2 functional for linear elastostatics can be presented as a sum of subdomain contributions:

$$\Pi_{\mathrm{HWM2}}(u_i, \varepsilon_{ij}, \sigma_{ij}, t_i, \lambda_{\mathrm{l}i}, u_{\mathrm{b}i}) = \Pi_{\mathrm{HW}} - \pi_u = \sum_m \Pi^m_{\mathrm{HW}} - \sum_m \pi^m_u \tag{2}$$

in which

$$\begin{aligned} \Pi^m_{\mathrm{HW}} &= \int_{\partial\Omega^m} [\mathscr{U}(\varepsilon^m_{ij}) + \sigma^m_{ij}(u^m_{(i,j)} - \varepsilon^m_{ij}) - u^m_i \bar{f}^m_i]\,\mathrm{d}\Omega - \int_{\partial\Omega^m_\sigma} u^m_i\, \bar{t}^m_i\,\mathrm{d}S - \int_{\partial\Omega^m_u} t^m_i\,(u^m_i - \bar{u}^m_i)\,\mathrm{d}S \\ \pi^m_u &= \int_{\partial\Omega^m_{\mathrm{b}}} \lambda^m_{\mathrm{l}i}(u^m_i - u_{\mathrm{b}i})\,\mathrm{d}S \end{aligned} \tag{3}$$

The sum over $m$ extends from 1 to the number of subdomains $N_{\mathrm{s}}$. For the boundary integrals $\mathrm{d}S$ is used to denote the boundary differential instead of the clumsier $\mathrm{d}\partial\Omega$. Note that $\Pi^m_{\mathrm{HW}}$, called the *interior functional* for obvious reasons, is fully subdomain localized since all entities have superscript $m$. The only interpartition connection is through $u_{\mathrm{b}i}$ in $\pi^m_u$, which is called an *interface potential* or *dislocation potential* in continuum mechanics. The sum of the $\pi^m_u$ results in the integral being carried out twice on each interface, once on each side of $\partial\Omega_{\mathrm{b}}$, as is typical of hybrid functionals. If the compatibility condition $u^m_i = u_{\mathrm{b}i}$ is enforced *a priori*, $\pi_u$ drops out and the ordinary Hu–Washizu functional $\Pi_{\mathrm{HW}}$ results. (The HW functional is expressable in two forms, which can be transformed from one to another through integration by parts.)

 

Atluri [6] shows that the stationarity condition $\delta\Pi_{\mathrm{HWM2}} = 0$ yields: (i) the elasticity field equations $\varepsilon_{ij} = u_{(i,j)}$, $\sigma_{ij} = E_{ijkl}\varepsilon_{kl}$ and $\sigma_{ij,j} + \bar{f}_i = 0$ in $\Omega$ as Euler equations; (ii) the displacement boundary condition $u_i = \bar{u}_i$ on $\partial\Omega_u$ and the traction boundary condition $\bar{t}_i = \sigma_{ij}n_j$ on $\partial\Omega_\sigma$ as natural boundary conditions; (iii) the interface compatibility $u_i = u_{\mathrm{b}i}$ and traction equilibrium $\lambda_{\mathrm{l}i} = t_i$ on $\partial\Omega_{\mathrm{b}}$ as interface continuity conditions.

The original objective for (3), as well as specializations thereof, was construction of finite elements. If the interface $\partial\Omega_{\mathrm{b}}$ surrounds each element, each subdomain collapses to an individual element. All interior fields: $u_i^m$, $\varepsilon_{ij}^m$ and $\sigma_{ij}^m$, as well as the multiplier field $\lambda_{\mathrm{l}i}^m$, are eliminated at the element level, leaving only the boundary frame displacement $u_{\mathrm{b}i}$ as primary unknown. This is the standard technique for constructing hybrid models. The resulting elements can be processed by FEM programs as if they were ordinary displacement models. For use of (3) in partitioned analysis, however, it will be found convenient to retain all boundary frame fields in the discrete equations.

### 3.2. Simplifications

We are primarily interested in the treatment of interface conditions rather than constructing new elements. Hence we begin by simplifying $\Pi_{\mathrm{HWM2}}$ in two respects:

1. The relations $\varepsilon_{ij} = u_{(i,j)}$ and $\sigma_{ij} = E_{ijkl}u_{(k,l)}$ in $\Omega$ are imposed *a priori*. This eliminates $\varepsilon_{ij}$ and $\sigma_{ij}$ as independently varied fields, and reduces the interior functional to the Potential Energy (PE) functional.
2. Prescribed displacement portions $\partial\Omega_u$ of $\partial\Omega$ are treated in the same way as $\partial\Omega_{\mathrm{b}}$. The traction field $t_i$ on those portions is identified with the multiplier field $\lambda_{\mathrm{l}i}$, as illustrated in Figure 2(c). This modification allows processing all subdomains as free–free (i.e., possessing a full set of rigid-body modes), which simplifies the computer implementation.

These changes reduce (2) to a modified form of the potential energy functional

$$\Pi_{\mathrm{PEM2}}(u_i, \lambda_{\mathrm{l}i}, u_{\mathrm{b}i}) = \Pi_{\mathrm{PE}} - \pi_u = \sum_m \Pi_{\mathrm{PE}}^m - \sum_m \pi_u^m \tag{4}$$

in which

$$\begin{aligned} \Pi_{\mathrm{PE}}^m &= \int_{\Omega^m} [\mathscr{U}(u_i^m) - u_i^m \bar{f}_i^m]\,\mathrm{d}\Omega - \int_{\partial\Omega_\sigma^m} u_i{}^m\, \bar{t}_i^m\,\mathrm{d}S \\ \pi_u^m &= \int_{\partial\Omega_{\mathrm{b}}^m \cup \partial\Omega_u^m} \lambda_{\mathrm{l}i}^m (u_i^m - u_{\mathrm{b}i})\,\mathrm{d}S \end{aligned} \tag{5}$$

To redefine $\pi_u$, the frame displacements $u_{bi}$ are formally extended so that $u_{\mathrm{b}i} = \bar{u}_i$ on $\partial\Omega_u$. The functional labeled $\Pi_{\mathrm{HD2}}$ by Atluri [6] is essentially $\Pi_{\mathrm{PEM2}}$, except for keeping the original integral over $\partial\Omega_u$ in the interior functional. That hybrid functional was originally proposed by Tong [28].

A related functional is the one that governs the unscaled free formulation [29, 30] of finite elements:

$$\Pi_{\mathrm{UFF}}(u_i, t_i, u_{\mathrm{b}i}) = \sum_m \left[ \int_{\Omega^m} [\mathscr{U}(u_i^m) - u_i^m \bar{f}_i^m]\,\mathrm{d}\Omega - \int_{\partial\Omega_\sigma^m} u_{\mathrm{b}i}^m\, \bar{t}_i^m\,\mathrm{d}S - \int_{\partial\Omega^m} t_i{}^m (u_i^m - u_{\mathrm{b}i})\,\mathrm{d}S \right] \tag{6}$$

 

The interface integral of $\Pi_{\mathrm{UFF}}$ extends over the *complete boundary* of each subdomain: $\partial\Omega^m : \partial\Omega^m_\sigma \cup \partial\Omega^m_u \cup \partial\Omega^m_{\mathrm{b}}$, as illustrated in Figure 2(d). This form can be obtained from (4) by extending $u_{\mathrm{b}i}$ and $\lambda_{\mathrm{l}i}$ to $\partial\Omega_\sigma$, adding and subtracting $\int_{\partial\Omega_\sigma} \lambda_{\mathrm{l}i}(u_i - u_{\mathrm{b}i})\,\mathrm{d}S$ and renaming $\lambda_{\mathrm{l}i} \to t_i$. Note that the $\partial\Omega^m_\sigma$ term in (6) involves $u_{\mathrm{b}i}$ and not $u^m_i$. This treatment of traction boundary conditions is more convenient for individual element formulations because in that case the internal displacements $u^m_i$ are eliminated at the element level. The Scaled FF functional contains a free parameter in the interior component that interpolates between the potential energy and Hellinger–Reissner forms [30].

### 3.3. Displacement decomposition

For several applications of partitioned analysis, notably inverse problems and parallel solution, it is convenient to explicitly separate the rigid-body modes in the governing equation of floating subdomains. Following de Veubeke [22] this is done by decomposing total displacements into deformational and rigid-body components:

$$u_i(x_k) = d_i(x_k) + r_i(x_k) \tag{7}$$

Since $u_{(i,j)} = d_{(i,j)}$ the strain energy density $\mathscr{U}$ becomes function of the deformational displacements $d_i$ only: $\mathscr{U}(d_i) = \frac{1}{2} E_{ijkl}\, d_{(i,j)}\, d_{(k,l)}$. Inserting (7) into (4) we obtain the four-field functional

$$\tilde{\Pi}_{\mathrm{PEM2}}(d_i, r_i, \lambda_{\mathrm{l}i}, u_{\mathrm{b}i}) = \tilde{\Pi}_{\mathrm{PE}} - \tilde{\pi}_u = \sum_m \tilde{\Pi}^m_{\mathrm{PE}} - \sum_m \tilde{\pi}^m_u \tag{8}$$

in which

$$\begin{aligned} \tilde{\Pi}^m_{\mathrm{PE}} &= \int_{\Omega^m} [\mathscr{U}(d^m_i) - (d^m_i + r^m_i)\bar{f}^m_i]\,\mathrm{d}\Omega - \int_{\partial\Omega^m_\sigma} (d^m_i + r^m_i)\bar{t}^m_i\,\mathrm{d}S \\ \tilde{\pi}^m_u &= \int_{\partial\Omega^m_{\mathrm{b}}} \lambda^m_{\mathrm{l}i}(d^m_i + r^m_i - u_{\mathrm{b}i})\,\mathrm{d}S \end{aligned} \tag{9}$$

### 3.4. Deformation-RBM orthogonality condition

Given a subdomain displacement field $u^m_i$, decomposition (7) is unique if the following orthogonality condition is imposed:

$$\int_{\Omega^m} d^m_i r^m_i\,\mathrm{d}\Omega = \int_{\Omega^m} (u^m_i - r^m_i)\, r^m_i\,\mathrm{d}\Omega = 0 \tag{10}$$

This can be shown as follows. Over each subdomain the rigid-body displacements can be expressed as

$$r^m_i = R^m_{ij}\,\alpha^m_j \tag{11}$$

where $\alpha^m_j$ are subdomain rigid-body mode (RBM) amplitudes and $R^m_{ij}$ are entries of a dimensionless full-rank matrix $\mathbf{R}^m$ whose columns span the RBMs. The entries of $\mathbf{R}^m$ are at most linear in the co-ordinates $x_i$. $\mathbf{R}^m$ is formed by selecting a linearly independent RBM basis for its columns, followed by orthonormalization: $\int_{\Omega^m} R^m_{ji} R^m_{ik} = V^m \delta_{jk}$, in which $\delta_{jk}$ is the Kronecker delta and $V^m = \int_{\Omega^m} \mathrm{d}\Omega$ is the subdomain volume (area, length). Substitution into the second of (10) yields

$$\left( \int_{\Omega^m} u^m_i R^m_{ij}\,\mathrm{d}\Omega - \alpha^m_k \int_{\Omega^m} R^m_{ki} R^m_{ij}\,\mathrm{d}\Omega \right) \alpha^m_j = (P^m_j - V^m \alpha^m_j)\,\alpha^m_j = 0 \tag{12}$$

 

where $P_j^m = \int_{\Omega^m} u_i^m R_{ij}^m \, \mathrm{d}\Omega$. The non-trivial solution of (12) is obtained by taking $\alpha_j^m = P_j^m / V^m$. We observe that the RBM amplitude $\alpha_j^m$ is merely the projection of the displacement $u_i^m$ on the $j$th rigid-body mode $R_{ij}^m$. If $\mathbf{R}^m$ is not orthonormalized the inverse of a weighting matrix appears in (12).

### 3.5. Stationarity conditions: static case

Varying $\Pi_{\mathrm{PEM2}}$ in the static case yields the weak (Galerkin) form

$$\delta\Pi_{\mathrm{PEM2}} = \sum_m \{ G_{\mathrm{d}i}^m \, \delta d_i^m + G_{\alpha i}^m \, \delta\alpha_i^m + G_{\lambda \mathrm{l} i}^m \, \delta\lambda_{\mathrm{l}i}^m + G_{u\mathrm{b}i}^m \, \delta u_{\mathrm{b}i} \} \tag{13}$$

in which account is taken of (11) to express $\delta r_j^m = R_{ji}^m \delta\alpha_i^m$. The subdomain variational coefficients are

$$\begin{aligned}
G_{\mathrm{d}i}^m &= \int_{\Omega^m} p_i^m \, \mathrm{d}\Omega - \int_{\Omega^m} \bar{f}_i^m \, \mathrm{d}\Omega - \int_{\partial\Omega_\sigma^m} \bar{t}_i^m \, \mathrm{dS} - \int_{\partial\Omega_{\mathrm{b}}^m} \lambda_{\mathrm{l}i}^m \, \mathrm{d}S \\
G_{\alpha i}^m &= -\int_{\Omega^m} \bar{f}_j^m \, R_{ij}^m \, \mathrm{d}\Omega - \int_{\partial\Omega_\sigma^m} \bar{t}_j^m \, R_{ij}^m \, \mathrm{dS} - \int_{\partial\Omega_{\mathrm{b}}^m} \lambda_{\mathrm{l}j}^m R_{ij}^m \, \mathrm{d}S \\
G_{\lambda \mathrm{l} i}^m &= -\int_{\partial\Omega_{\mathrm{b}}^m} [d_i^m + r_i^m - u_{\mathrm{b}i}] \, \mathrm{d}S \\
G_{u\mathrm{b}i}^m &= -\int_{\partial\Omega_{\mathrm{b}}^m} \lambda_{\mathrm{l}i}^m \, \mathrm{d}S
\end{aligned} \tag{14}$$

In the first of (14), $p_i^m$ is the internal force density that results from the variation of the internal energy density: $\delta\mathscr{U}^m = p_i^m \, \delta d_i^m$. Setting variation (13) to zero provides weak forms of deformational equilibrium, rigid-body equilibrium, interface compatibility (including prescribed displacements) and interface equilibrium (Newton's third law at subdomain boundaries) conditions, respectively. The first two are *localized* at the subdomain level. The only connection between subdomains is done through the last two conditions, which bring in the partition frame displacements $u_{\mathrm{b}i}$.

### 3.6. Stationarity conditions: dynamic case

Functional (10) can be formally extended to dynamic problems through the substitution of $\bar{f}_i$ by the D'Alembert's force

$$f_i = \bar{f}_i - \rho(\ddot{d}_i + \ddot{r}_i) \tag{15}$$

With this replacement $\delta\tilde{\Pi}_{\mathrm{PEM2}} = 0$ is a restricted variational principle in which time is to be held frozen on variation. We note that, if desired, it can be transformed to a Hamiltonian principle through integration by parts of the kinetic energy terms.

Substitution (15) produces kinetic energy density terms in the four combinations $\rho r_i \ddot{r}_i$, $\rho d_i \ddot{r}_i$, $\rho \ddot{d}_i r_i$ and $\rho r_i \ddot{r}_i$. If $\rho$ is constant, enforcing the orthogonality condition (10) makes the cross-coupling terms $d_i \ddot{r}_i$ and $\ddot{d}_i r_i$ vanish on integration over $\Omega^m$. If $\rho$ is not constant over the subdomain, however, (10) must be modified with the mass density as weight function

$$\int_{\Omega^m} \rho^m \, d_i^m \, r_i^m \, \mathrm{d}\Omega = \int_{\Omega^m} \rho^m \, (u_i^m - r_i^m) \, r_i^m \, \mathrm{d}\Omega = 0 \tag{16}$$

 

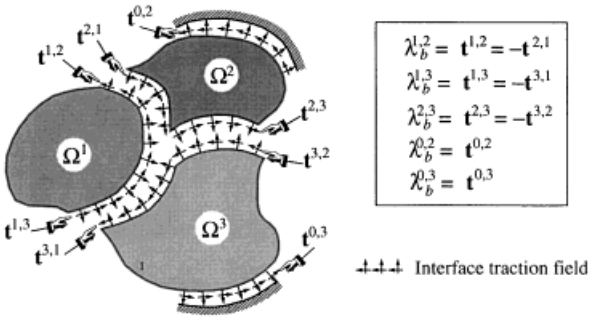


Figure 3. Direct subdomain connection using global Lagrange multipliers

This results in simple modifications to the integrals of (12). Assuming this 'mass orthogonality' is enforced, the restricted variation (with frozen time) leads again to the weak form (13), in which the first two coefficients are augmented with acceleration terms:

$$G_{\mathrm{d}i}^m = \int_{\Omega^m} p_i^m \,\mathrm{d}\Omega - \int_{\Omega^m} (\bar{f}_i^m - \rho^m \ddot{d}_i^m)\,\mathrm{d}\Omega - \int_{\partial\Omega_\sigma^m} \bar{t}_i^m \,\mathrm{d}S - \int_{\partial\Omega_{\mathrm{b}}^m} \lambda_{\mathrm{l}i}^m \,\mathrm{d}S$$
$$G_{\alpha i}^m = -\int_{\Omega^m} (\bar{f}_j^m R_{ij}^m - \rho^m R_{ij}^m \ddot{\alpha}_j^m)\,\mathrm{d}\Omega - \int_{\partial\Omega_\sigma^m} \bar{t}_j^m R_{ij}^m \,\mathrm{d}S - \int_{\partial\Omega_{\mathrm{b}}^m} \lambda_{\mathrm{l}i}^m R_{ij}^m \,\mathrm{d}S \tag{17}$$

### 3.7. Connection through global Lagrange multipliers

As noted in the historical remarks of Section 2, in the classical method of Lagrange multipliers developed originally for particle and celestial mechanics, constrained bodies are directly connected by interaction forces. The equivalent technique for partitioned analysis is illustrated in Figure 3. The partition frame $\partial\Omega_{\mathrm{b}}$ that effectively localizes the Lagrange multipliers is omitted. Compatibility of boundary displacements of two connected subdomains, $m$ and $n$, is enforced by traction fields $t_i^{m,n}$ and $t_i^{n,m}$, which satisfy Newton's third law $t_i^{m,n} + t_i^{n,m} = 0$. To avoid carrying over two sets of tractions, a *from-to sign convention* must be established. For each pair $\{m,n\}$ of linked subdomains, we choose the traction flow as positive from $m$ to $n$ if $m < n$. The global multiplier field $\lambda_{\mathrm{b}i}^{m,n}$ is defined as $\lambda_{\mathrm{b}i}^{m,n} = t_i^{m,n} = -t_i^{n,m}$ for $m < n$. This rule can be subsumed into one equation using an alternator symbol

$$\lambda_{\mathrm{b}i}^{m,n} = c^{m,n}\, t_i^{m,n}, \quad \text{in which} \quad c^{m,n} = \begin{cases} 0 & \text{if } m = n \text{ or } \{m,n\} \text{ are not connected} \\ +1 & \text{if } m < n \\ -1 & \text{if } m > n \end{cases} \tag{18}$$

The notation is extended to include the prescribed displacement portions by conventionally identifying the ground as subdomain zero (see Figure 3). Hence $m$ ranges from 0 to the number of subdomains $N_{\mathrm{s}}$. The variational form of this technique is based on the hybrid functional

$$\Pi_{\mathrm{PEM1}}(u_i, \lambda_{\mathrm{b}i}) = \Pi_{\mathrm{PE}} - \pi_\lambda \tag{19}$$

 

where $\Pi_{\mathrm{PE}}$ is the same as in $\Pi_{\mathrm{PEM2}}$, and

$$\pi_\lambda = \int_{\partial\Omega_{\mathrm{b}}} \lambda_{\mathrm{b}i}\, u_i \,\mathrm{d}S = \sum_{m=0}^{N_{\mathrm{s}}} \sum_{n=1}^{N_{\mathrm{s}}} \int_{\partial\Omega_{\mathrm{b}}^{m,n}} c^{m,n}\, t_i^{m,n}\, u_i^m \,\mathrm{d}S \tag{20}$$

This interface potential was first proposed by Prager [27] to treat internal physical discontinuities. If coupled with $\Pi_{\mathrm{HW}}$, a functional similar to $\Pi_{\mathrm{HWM1}}$ of Atluri [6] results but for the different treatment of $\partial\Omega_u$. Inserting the decomposition $u_i = d_i + r_i$ into $\Pi_{\mathrm{PEM1}}$ yields

$$\tilde{\Pi}_{\mathrm{PEM1}}(r_i, d_i, \lambda_{\mathrm{b}i}) = \tilde{\Pi}_{\mathrm{PE}} + \tilde{\pi}_\lambda \tag{21}$$

where

$$\tilde{\pi}_\lambda = \int_{\partial\Omega_{\mathrm{b}}} \lambda_{\mathrm{b}i}\,(d_i + r_i)\,\mathrm{d}S = \sum_{m=0}^{N_{\mathrm{s}}} \sum_{n=1}^{N_{\mathrm{s}}} \int_{\partial\Omega_{\mathrm{b}}^{m,n}} c^{m,n}\, t_i^{m,n}\,(d_i^m + r_i^m)\,\mathrm{d}S \tag{22}$$

The variation of $\tilde{\Pi}_{\mathrm{PEM1}}$ in the static case yields the weak form

$$\delta\tilde{\Pi}_{\mathrm{PEM1}} = \sum_m \{G_{\mathrm{d}i}^m\, \delta d_i + G_{\alpha i}^m\, \delta\alpha_i^m\} + \sum_m \sum_n G_{\lambda i}^{m,n}\, \delta\lambda_{\mathrm{b}i} \tag{23}$$

where

$$\begin{aligned}
G_{\mathrm{d}i}^m &= \int_{\Omega^m} p_i^m \,\mathrm{d}\Omega - \int_{\Omega^m} \bar{f}_i^m \,\mathrm{d}\Omega - \int_{\partial\Omega_\sigma^m} \bar{t}_i^m \,\mathrm{d}S - \int_{\partial\Omega_{\mathrm{b}}^m} \lambda_{\mathrm{b}i} \,\mathrm{d}S \\
G_{\alpha i}^m &= -\int_{\Omega^m} \bar{f}_j^m R_{ij}^m \,\mathrm{d}\Omega - \int_{\partial\Omega_\sigma^m} \bar{t}_j^m R_{ij}^m \,\mathrm{d}S - \int_{\partial\Omega_{\mathrm{b}}^m} \lambda_{\mathrm{b}j}\, R_{ij}^m \,\mathrm{d}S \\
G_{\lambda i}^{m,n} &= -\int_{\partial\Omega_{\mathrm{b}}^{m,n}} c^{m,n}(d_i^m + r_i^m)\,\mathrm{d}S
\end{aligned} \tag{24}$$

Generalization to the dynamic case can be carried out as in the case of $\tilde{\Pi}_{\mathrm{PEM2}}$.

## 4. TREATMENT OF NON-MATCHING MESHES

As noted in the Introduction, non-matching meshes can arise from a variety of sources: separately constructed discretizations, localized refinement, global–local analysis and coupled-field problems. Functionals (4) and (8) provide adequate tools to treat non-matching meshes of mechanical finite elements. This section discusses aspects of the discretization procedure associated with the use of Lagrange multipliers. It should be noted that primal techniques that do not use multipliers, such as the 'mortar method' of Bernardi *et al.* [31], have been recently developed to couple non-matching meshes. Such techniques are appropriate when master and slaves interfaces can be readily identified; for example a fine mesh linked to a coarse one as is common in global–local analysis.

For definiteness the discussion refers to the case illustrated in Figure 4. Upon discretization the nodes on the partition frame $\partial\Omega_{\mathrm{b}}$ neither match those on subdomain $\Omega^1$ nor subdomain $\Omega^2$. The two interface methods depicted there correspond to the functionals $\Pi_{\mathrm{PEM2}}$ and $\Pi_{\mathrm{PEM1}}$, respectively.

 

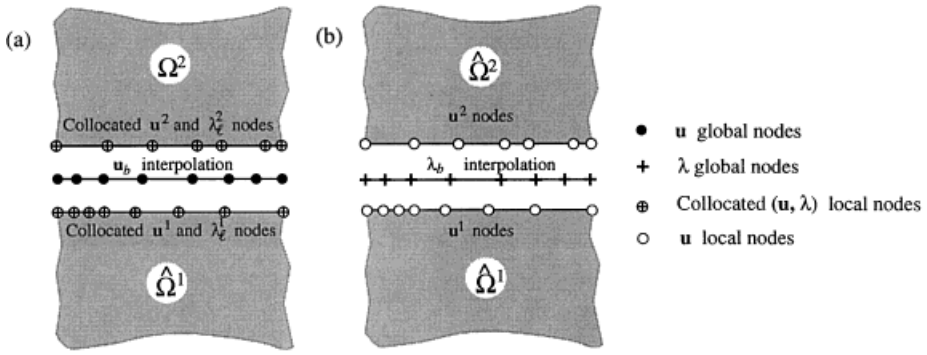


Figure 4. Two connection schemes for non-matched mesh interfaces: (a) connection by global displacements and node-force-collocated local multipliers; (b) connection by global multipliers

Throughout this Section the displacement field is kept as $u_i$, without decomposing into $r_i$ and $d_i$, to clarify the exposition. The more general case is dealt with in Section 5.

The continuum interface potential for the localized functional (5) is given by

$$\pi_u(u_i^1, u_i^2, \lambda_{1i}^1, \lambda_{1i}^2, u_{bi}) = \int_{\partial\Omega^1} \lambda_{1i}^1 u_i^1 \,\mathrm{d}S + \int_{\partial\Omega^2} \lambda_{1i}^2 u_i^2 \,\mathrm{d}S - \int_{\partial\Omega_b^1} \lambda_{1i}^1 u_{bi} \,\mathrm{d}S - \int_{\partial\Omega_b^2} \lambda_{1i}^2 u_{bi} \,\mathrm{d}S \tag{25}$$

In the above expressions, $\partial\Omega_b^1$ denotes the projection of the attributes on $\partial\Omega^1$ onto $\partial\Omega_b$, and similarly for $\partial\Omega_b^2$.

The continuum interface potential for the global functional (18) is given by

$$\pi_\lambda(u_i^1, u_i^2, \lambda_{bi}) = \int_{\partial\Omega_b^1} \lambda_{bi} u_i^1 \,\mathrm{d}S - \int_{\partial\Omega_b^2} \lambda_{bi} u_i^2 \,\mathrm{d}S \tag{26}$$

### *4.1. Discretization by localized multipliers*

The FEM interpolations assumed for the case of Figure 4(a) are

$$\{u^1\} = \mathbf{N}_u^1 \mathbf{u}^1, \quad \{u^2\} = \mathbf{N}_u^2 \mathbf{u}^2, \quad \{\lambda^1\} = \mathbf{N}_\lambda^1 \boldsymbol{\lambda}^1, \quad \{\lambda^2\} = \mathbf{N}_\lambda^2 \boldsymbol{\lambda}^2, \quad \{u_b\} = \mathbf{N}_u^b \mathbf{u}_b \tag{27}$$

where $\mathbf{N}_u^1$, for example, collects the shape functions of the interface displacement $\{u^1\}$. If the example of Figure 4 corresponds to plane stress, $\mathbf{N}_u^1$ would be a $2 \times 16$ matrix, since there are then two displacement components ($i = 1, 2$) and eight nodes on the $\Omega^1$ interface; matrices $\mathbf{N}_u^2$, $\mathbf{N}_\lambda^1$, $\mathbf{N}_\lambda^2$ and $\mathbf{N}_u^b$ would be dimensioned $2 \times 14$, $2 \times 16$, $2 \times 14$ and $2 \times 16$, respectively.

Substituting these interpolations into (25) the discrete version results:

$$\hat{\pi}_u(\mathbf{u}^1, \mathbf{u}^2, \boldsymbol{\lambda}^1, \boldsymbol{\lambda}^2, \mathbf{u}_b) = (\boldsymbol{\lambda}^1)^{\mathrm{T}} (\mathbf{C}_1 \mathbf{u}^1 - \mathbf{C}_{1b} \mathbf{u}_b) + (\boldsymbol{\lambda}^2)^{\mathrm{T}} (\mathbf{C}_2 \mathbf{u}^2 - \mathbf{C}_{2b} \mathbf{u}_b) \tag{28}$$

in which the $\mathbf{C}$ are connection matrices (also called constraint matrices):

$$\mathbf{C}_k = \int_{\partial\Omega^k} (\mathbf{N}_\lambda^k)^{\mathrm{T}} \mathbf{N}_u^k \,\mathrm{d}S, \quad \mathbf{C}_{kb} = \int_{\partial\Omega_b^k} (\mathbf{N}_\lambda^k)^{\mathrm{T}} \mathbf{N}_u^b \,\mathrm{d}S, \quad k = 1, 2 \tag{29}$$

The simplest choice for multiplier interpolation is *node-force collocation*, in which the multipliers are simply point (concentrated) forces at multiplier nodes that coincide with the local displacement

 

nodes. This choice is that depicted in Figure 4(a) by merging cross and circle symbols. Matrices $\mathbf{N}_\lambda^1$ and $\mathbf{N}_\lambda^2$ consist of delta functions collocated at the subdomain mesh nodes. If so, $\mathbf{C}_1$ and $\mathbf{C}_2$ reduce to identity matrices whereas the entries of $\mathbf{C}_{1\mathrm{b}}$ and $\mathbf{C}_{2\mathrm{b}}$ are obtained simply by evaluating $\mathbf{N}_u^{\mathrm{b}}$ at interface nodes. Furthermore, the interface force vector associated with the multiplier nodal values is simply

$$\mathbf{f}_{\mathrm{b}} = \begin{bmatrix} \dfrac{\partial \hat{\pi}_u}{\partial \mathbf{u}^1} \\ \dfrac{\partial \hat{\pi}_u}{\partial \mathbf{u}^2} \end{bmatrix} = \begin{bmatrix} \boldsymbol{\lambda}^1 \\ \boldsymbol{\lambda}^2 \end{bmatrix} \tag{30}$$

Consequently, full domain discretization accuracy is preserved. Another advantage of the node-force-collocated multiplier discretization is the fact that $\mathbf{N}_u^1$ and $\mathbf{N}_u^2$ do not appear in the connection matrices. Hence the implementor of a partitioned analysis program need not know the types of finite element that are being linked. This feature helps software modularity.

If collocation is adopted, there still remains the problem of interpolating the frame displacements. As a general guideline, if the number of interface nodes on subdomains $\Omega^1$ and $\Omega^2$ is $n_1$ and $n_2$, respectively, the number of global displacement nodes, marked by a dark circle in Figure 4(a), should be at least $\max(n_1, n_2)$. This rule does not tell, however, how those nodes should be placed. This is the subject of current research.

If the meshes match, that is, when all nodes are collocated and the multipliers are node forces, the connection matrices reduce to Boolean matrices with 0 or 1 entries.

### *4.2. Discretization by globalized multipliers*

For the globalized multiplier case the FEM interpolation is

$$\{u^1\} = \mathbf{N}_u^1 \mathbf{u}^1, \quad \{u^2\} = \mathbf{N}_u^2 \mathbf{u}^2, \quad \{\lambda_{\mathrm{b}}\} = \mathbf{N}_\lambda^{\mathrm{b}} \mathbf{u}_i \tag{31}$$

where $\mathbf{N}_\lambda^{1,2}$ is constructed from the multiplier nodes marked by a cross in Figure 4(b). The rules for selecting such nodes are more delicate than in the previous case. The discretized interface functional is

$$\hat{\pi}_\lambda(\mathbf{u}^1, \mathbf{u}^2, \boldsymbol{\lambda}_{\mathrm{b}}) = (\boldsymbol{\lambda}_{\mathrm{b}})^{\mathrm{T}} (\mathbf{C}_{\lambda 1} \mathbf{u}^1 - \mathbf{C}_{\lambda 2} \mathbf{u}^2) \tag{32}$$

in which

$$\mathbf{C}_{\lambda 1} = \int_{\partial\Omega_{\mathrm{b}}} (\mathbf{N}_\lambda^{\mathrm{b}})^{\mathrm{T}} \mathbf{N}_u^1 \, \mathrm{d}S, \quad \mathbf{C}_{\lambda 2} = \int_{\partial\Omega_{\mathrm{b}}} (\mathbf{N}_\lambda^{\mathrm{b}})^{\mathrm{T}} \mathbf{N}_u^2 \, \mathrm{d}S \tag{33}$$

Again, should $\lambda_{\mathrm{b}}$ be defined by point forces at multiplier nodes the connection matrices can be simply constructed by evaluating $\mathbf{N}_u^1$ and $\mathbf{N}_u^2$ at the multiplier nodes. The displacement interpolation, however, would depend on the type of element adjacent to the interface. This hinders software modularity.

The interface force vector associated with the multiplier nodal values is

$$\mathbf{f}_{\mathrm{b}} = \begin{bmatrix} \dfrac{\partial \hat{\pi}_\lambda}{\partial \mathbf{u}^1} \\ \dfrac{\partial \hat{\pi}_\lambda}{\partial \mathbf{u}^2} \end{bmatrix} = \begin{bmatrix} \mathbf{C}_{\lambda 1} \boldsymbol{\lambda}^1 \\ -\mathbf{C}_{\lambda 2} \boldsymbol{\lambda}^2 \end{bmatrix} \tag{34}$$

 

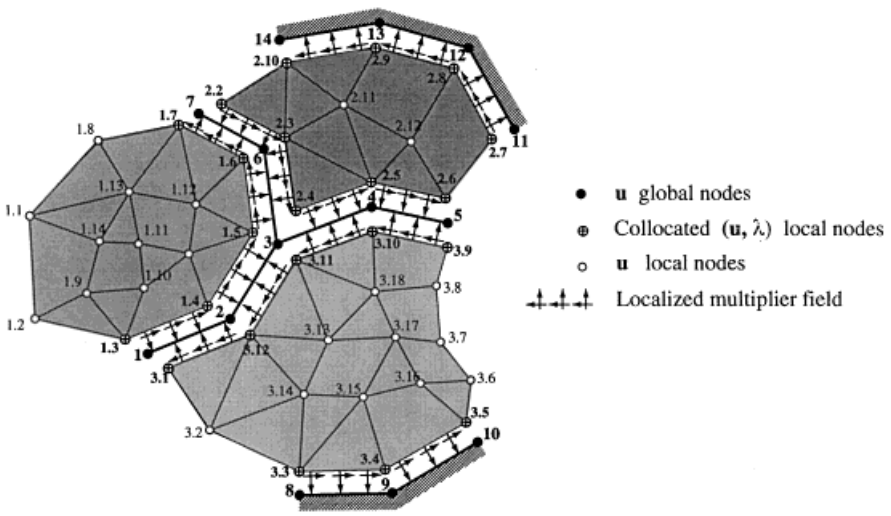


Figure 5. Localized-multiplier FEM discretization of example domain of Figure 1(c). Matched submeshes shown for simplicity. Three node types are identified by indicated symbols. Prescribed displacement portions of the boundary are treated as internal interfaces. Global nodes conventionally belong to subdomain zero. Hence node numbers $1, 2, \ldots$ could have also been identified $0{\cdot}1, 0{\cdot}2, \ldots$, should that simplify the implementation

On studying expressions (30) and (34) for the interface forces, we find that in the former there emerges a least-squares projection operator that plays the role of filtering out the boundary frame modes. This property enforces Newton's action–reaction law in a least-square sense. On the other hand, there is no *a priori* guarantee that the law would be satisfied by (34). Preliminary numerical experiments corroborate these remarks.

If the meshes match and node-force collocation is used for $\lambda_b$, the connection matrices become incident matrices, with entries $\pm 1$ or 0. Note that these are no longer Boolean matrices.

## 5. FEM DISCRETIZATION

We now pass to consider the displacement-based FEM discretization of the $\Pi_{PEM2}$ functional. A typical configuration of the resulting discretization is illustrated in Figure 5. Although a matched mesh is shown for visualization convenience, the development that follows is valid for non-matching meshes. Three types of node points illustrated in Figure 5 should be distinguished:

1. Global interface nodes, or $\mathbf{u}_b$ nodes, which define the interpolation on $\partial\Omega_b$ and $\partial\Omega_u$. These are numbered 1–14 in Figure 5. Conventionally these belong to subdomain zero.
2. Local interface nodes or $(\mathbf{u}, \lambda)$ nodes, which for matched meshes are paired with the global nodes on $\partial\Omega_b$ and $\partial\Omega_u$. For example, local nodes $2{\cdot}5$ and $3{\cdot}10$ are paired to global node 4.
3. Local nodes, or $\mathbf{u}$ nodes, are all nodes that do not fit the previous two types. These are located either on the inside of the subdomain meshes, or on $\mathbf{S}_\sigma$; e.g. nodes $1{\cdot}11$ and $3{\cdot}2$ in Figure 5.

 

For a problem with $n_{\mathrm{f}}$ displacement freedoms per node, these node types carry $2n_{\mathrm{f}}$, $2n_{\mathrm{f}}$ and $n_{\mathrm{f}}$ freedoms, respectively.

For non-matching meshes it may be necessary to consider four node types if multiplier and displacement freedoms on partition boundaries do not coincide. The fourth type includes the so-called 'multiplier nodes' or $\lambda$ nodes, which are identified by a cross symbol.

### 5.1. Localized multiplier system equations

The component-by-component interpolations of subdomain quantities are

$$d_i^m = \mathbf{N}_{\mathrm{d}i}^m \mathbf{d}^m, \quad r_i^m = \mathbf{R}_i^m \boldsymbol{\alpha}^m, \quad \lambda_{\mathrm{l}i}^m = \mathbf{N}_{\lambda i}^m \boldsymbol{\lambda}_{\mathrm{l}}^m, \quad \bar{t}_i^m = \mathbf{N}_{ti}^m \bar{\mathbf{t}}^m, \quad \bar{f}_i^m = \mathbf{N}_{\mathrm{f}i}^m \bar{\mathbf{f}}^m \tag{35}$$

whereas displacement components of the partition frame are interpolated globally

$$u_{\mathrm{b}i} = \mathbf{N}_{\mathrm{b}i} \mathbf{u}_{\mathrm{b}} \tag{36}$$

Grouping these components gives the complete field interpolations

$$\begin{aligned} \{d^m\} &= \mathbf{N}_{\mathrm{d}}^m \mathbf{d}^m, \quad \{r^m\} = \mathbf{R}^m \boldsymbol{\alpha}^m \quad \{\lambda_{\mathrm{l}}^m\} = \mathbf{N}_{\lambda}^m \boldsymbol{\lambda}_{\mathrm{l}}^m \\ \{\bar{t}^m\} &= \mathbf{N}_t{}^m \bar{\mathbf{t}}^m, \quad \{\bar{f}^m\} = \mathbf{N}_{\mathrm{f}}^m \mathbf{f}^m, \quad \{u_{\mathrm{b}}\} = \mathbf{N}_{\mathrm{b}} \mathbf{u}_{\mathrm{b}} \end{aligned} \tag{37}$$

Here array $\mathbf{N}_{\mathrm{d}}^m$ collects the shape functions for the deformational displacement in subdomain $m$, and similarly for the others. Node values are stacked in subdomain arrays $\mathbf{d}^m$, $\boldsymbol{\lambda}^m$, $\bar{\mathbf{t}}^m$ and $\bar{\mathbf{f}}^m$, and in the global array $\mathbf{u}_{\mathrm{b}}$. For example, if Figure 5 represents a plane stress mesh, $\mathbf{d}^m$ and $\boldsymbol{\lambda}^m$ have dimension 38 and 16, respectively, for $m = 2$, whereas $\mathbf{u}_{\mathrm{b}}$ has dimension 28. Prescribed displacements, if any, are included in the interpolation of $\{u_{\mathrm{b}}\}$.

The interpolation for the subdomain rigid-body displacements, $\{r^m\} = \mathbf{R}^m \boldsymbol{\alpha}^m$, is special in that $\boldsymbol{\alpha}^m$ are nodeless variables associated with a subdomain rather than a node. For example, if Figure 5 is a plane stress mesh, each subdomain has three RBMs, $\boldsymbol{\alpha}^m$ has dimension 3 and $\mathbf{R}^m$ is $2 \times 3$ for each $m = 1, 2, 3$. We shall assume that the deformational-RBM orthogonality condition (16) is also enforced over each discretized subdomain.

The strain interpolation can be expressed as $\{\varepsilon^m\} = \mathbf{S}^m \mathbf{d}^m$, where the strain–displacement matrix $\mathbf{S}^m$ is constructed from the symmetric gradient of $\mathbf{N}_{\mathrm{d}}^m$. The stress interpolation is $\{\sigma^m\} = \mathbf{E}^m \{\varepsilon^m\}$, where $\mathbf{E}^m$ collects the constitutive moduli in matrix form.

Substituting these interpolations into $\Pi_{\mathrm{PEM2}}$ produces the discrete functional:

$$\hat{\Pi}_{\mathrm{PEM2}}(\mathbf{d}, \boldsymbol{\alpha}, \boldsymbol{\lambda}_{\mathrm{l}}, \mathbf{u}_{\hat{b}}, ) = \sum_m \left[ \hat{\Pi}_{\mathrm{PEM2a}}^m (\mathbf{d}^m, \boldsymbol{\alpha}^m, \lambda_{\mathrm{l}}^m) - \hat{\Pi}_{\mathrm{PEM2b}}^m (\boldsymbol{\lambda}_{\mathrm{l}}^m, \mathbf{u}_{\mathrm{b}}) \right] \tag{38}$$

The splitting (38) does not correspond to $\Pi_{\mathrm{PE}}^m + \pi_u^m$, but simplifies the physical visualization of the discrete equations. Here

$$\hat{\Pi}_{\mathrm{PEM2a}}^m = \begin{bmatrix} \mathbf{d}^m \\ \boldsymbol{\alpha}^m \\ \boldsymbol{\lambda}_{\mathrm{l}}^m \end{bmatrix}^{\mathrm{T}} \left\{ \frac{1}{2} \begin{bmatrix} \mathbf{K}_{\mathrm{dd}}^m & \mathbf{0} & \mathbf{B}_{\mathrm{d}\lambda}^m \\ \mathbf{0} & \mathbf{0} & \mathbf{R}_{\alpha\lambda}^m \\ \mathbf{B}_{\lambda\mathrm{d}}^m & \mathbf{R}_{\lambda\alpha}^m & \mathbf{0} \end{bmatrix} \begin{bmatrix} \mathbf{d}^m \\ \boldsymbol{\alpha}^m \\ \boldsymbol{\lambda}_{\mathrm{l}}^m \end{bmatrix} + \frac{1}{2} \begin{bmatrix} \mathbf{M}_{\mathrm{dd}}^m & \mathbf{0} & \mathbf{0} \\ \mathbf{0} & \mathbf{M}_{\alpha\alpha}^m & \mathbf{0} \\ \mathbf{0} & \mathbf{0} & \mathbf{0} \end{bmatrix} \begin{bmatrix} \ddot{\mathbf{d}}^m \\ \ddot{\boldsymbol{\alpha}}^m \\ \ddot{\boldsymbol{\lambda}}_{\mathrm{l}}^m \end{bmatrix} - \begin{bmatrix} \mathbf{f}_{\mathrm{d}}^m \\ \mathbf{f}_{\alpha}^m \\ \mathbf{0} \end{bmatrix} \right\} \tag{39}$$

 

represents the contribution of the $m$th subdomain plus the action of localized multipliers on its internal fields, whereas

$$\hat{\Pi}^m_{\mathrm{PEM2b}} = \begin{bmatrix} \boldsymbol{\lambda}^m_{\mathrm{l}} \\ \mathbf{u}^m_{\mathrm{b}} \end{bmatrix}^{\mathrm{T}} \begin{bmatrix} \mathbf{0} & \mathbf{C}^m_{\lambda u} \\ \mathbf{C}^m_{u\lambda} & \mathbf{0} \end{bmatrix} \begin{bmatrix} \boldsymbol{\lambda}^m \\ \mathbf{u}^m_{\mathrm{b}} \end{bmatrix} = \begin{bmatrix} \boldsymbol{\lambda}^m_{\mathrm{l}} \\ \mathbf{u}_{\mathrm{b}} \end{bmatrix}^{\mathrm{T}} \begin{bmatrix} \mathbf{0} & \mathbf{C}^m_{\lambda u}\mathbf{B}^m_{\mathrm{b}} \\ (\mathbf{B}^m_{\mathrm{b}})^{\mathrm{T}}\mathbf{C}^m_{u\lambda} & \mathbf{0} \end{bmatrix} \begin{bmatrix} \boldsymbol{\lambda}^m \\ \mathbf{u}_{\mathrm{b}} \end{bmatrix} \tag{40}$$

represents the contribution of the partition frame displacements. In (40), $\mathbf{u}^m_{\mathrm{b}} = \mathbf{B}^m_{\mathrm{b}}\mathbf{u}_{\mathrm{b}}$ is the portion of $\mathbf{u}_{\mathrm{b}}$ that contributes to subdomain $m$ and $\mathbf{B}^m_{\mathrm{b}}$ is the Boolean matrix that restricts $\mathbf{u}_{\mathrm{b}}$ to $\mathbf{u}^m_{\mathrm{b}}$.

The matrices and vectors appearing in (39)–(40) have the following expressions:

$$\begin{aligned}
\mathbf{K}^m_{\mathrm{dd}} &= \int_{\Omega^m} (\mathbf{S}^m)^{\mathrm{T}}\,\mathbf{E}^m\mathbf{S}^m\,\mathrm{d}\Omega, \qquad \mathbf{B}^m_{\mathrm{d}\lambda} = \int_{\partial\Omega^m_{\mathrm{b}}} (\mathbf{N}^m_{\mathrm{d}})^{\mathrm{T}}\,\mathbf{N}^m_{\lambda}\,\mathrm{d}\Omega = (\mathbf{B}^m_{\lambda\mathrm{d}})^{\mathrm{T}} \\
\mathbf{M}^m_{\mathrm{dd}} &= \int_{\Omega^m} \rho^m\,(\mathbf{N}^m_{\mathrm{d}})^{\mathrm{T}}\,\mathbf{N}^m_{\mathrm{d}}\,\mathrm{d}\Omega, \qquad \mathbf{R}^m_{\alpha\lambda} = \int_{\partial\Omega^m_{\mathrm{b}}} (\mathbf{R}^m)^{\mathrm{T}}\,\mathbf{N}^m_{\lambda}\,\mathrm{d}S = (\mathbf{R}^m_{\lambda\alpha})^{\mathrm{T}} \\
\mathbf{M}^m_{\alpha\alpha} &= \int_{\Omega^m} \rho^m\,(\mathbf{R}^m)^{\mathrm{T}}\,\mathbf{R}^m\,\mathrm{d}\Omega, \qquad \mathbf{C}^m_{u\lambda} = \int_{\partial\Omega^m_{\mathrm{b}}} \mathbf{N}^{\mathrm{T}}_{u}\,\mathbf{N}^m_{\lambda}\,\mathrm{d}\Omega = (\mathbf{C}^m_{\lambda u})^{\mathrm{T}} \\
\mathbf{f}^m_{\mathrm{d}} &= \int_{\Omega^m} (\mathbf{N}^m_{\mathrm{d}})^{\mathrm{T}}\,\mathbf{N}^m_{f}\,\mathrm{d}\Omega\,\bar{\mathbf{f}}^m + \int_{\partial\Omega^m_{\sigma}} (\mathbf{N}^m_{\mathrm{d}})^{\mathrm{T}}\,\mathbf{N}^m_{t}\,\mathrm{d}S\,\bar{\mathbf{t}}^m \\
\mathbf{f}^m_{\alpha} &= \int_{\Omega^m} (\mathbf{R}^m)^{\mathrm{T}}\,\mathbf{N}^m_{f}\,\mathrm{d}\Omega\,\bar{\mathbf{f}}^m + \int_{\partial\Omega^m_{\sigma}} (\mathbf{R}^m)^{\mathrm{T}}\,\mathbf{N}^m_{t}\,\mathrm{d}S\,\bar{\mathbf{t}}^m
\end{aligned} \tag{41}$$

Setting $\delta\hat{\Pi}^m_{\mathrm{PEM2}} = 0$ yields the discrete governing equations for each subdomain

$$\begin{bmatrix} \mathbf{K}^m_{\mathrm{dd}} & \mathbf{0} & \mathbf{B}^m_{\mathrm{d}\lambda} & \mathbf{0} \\ \mathbf{0} & \mathbf{0} & \mathbf{R}^m_{\alpha\lambda} & \mathbf{0} \\ \mathbf{B}^m_{\lambda\mathrm{d}} & \mathbf{R}^m_{\lambda\alpha} & \mathbf{0} & -\mathbf{C}^m_{\lambda u} \\ \mathbf{0} & \mathbf{0} & -\mathbf{C}^m_{u\lambda} & \mathbf{0} \end{bmatrix} \begin{bmatrix} \mathbf{d}^m \\ \boldsymbol{\alpha}^m \\ \boldsymbol{\lambda}^m_{\mathrm{l}} \\ \mathbf{u}^m_{\mathrm{b}} \end{bmatrix} + \begin{bmatrix} \mathbf{M}^m_{\mathrm{dd}} & \mathbf{0} & \mathbf{0} & \mathbf{0} \\ \mathbf{0} & \mathbf{M}^m_{\alpha\alpha} & \mathbf{0} & \mathbf{0} \\ \mathbf{0} & \mathbf{0} & \mathbf{0} & \mathbf{0} \\ \mathbf{0} & \mathbf{0} & \mathbf{0} & \mathbf{0} \end{bmatrix} \begin{bmatrix} \ddot{\mathbf{d}}^m \\ \ddot{\boldsymbol{\alpha}}^m \\ \ddot{\boldsymbol{\lambda}}^m_{\mathrm{l}} \\ \ddot{\mathbf{u}}^m_{\mathrm{b}} \end{bmatrix} = \begin{bmatrix} \mathbf{f}^m_{\mathrm{d}} \\ \mathbf{f}^m_{\alpha} \\ \mathbf{0} \\ \mathbf{0} \end{bmatrix} \tag{42}$$

The complete node value vectors $\mathbf{d}, \boldsymbol{\alpha}, \boldsymbol{\lambda}_{\mathrm{l}}$ are obtained by stacking up the contributions of the $N_{\mathrm{s}}$ subdomains

$$\mathbf{d} = \begin{bmatrix} \mathbf{d}^1 \\ \vdots \\ \mathbf{d}^{N_{\mathrm{s}}} \end{bmatrix}, \quad \boldsymbol{\alpha} = \begin{bmatrix} \boldsymbol{\alpha}^1 \\ \vdots \\ \boldsymbol{\alpha}^{N_{\mathrm{s}}} \end{bmatrix}, \quad \boldsymbol{\lambda}_{\mathrm{l}} = \begin{bmatrix} \boldsymbol{\lambda}^1 \\ \vdots \\ \boldsymbol{\lambda}^{N_{\mathrm{s}}} \end{bmatrix} \tag{43}$$

To establish the complete system equations in terms of the above relations, stack all subdomain matrices in block diagonal form, and link $\mathbf{u}^m_{\mathrm{b}} = \mathbf{B}^m_{\mathrm{b}}\mathbf{u}_{\mathrm{b}}$:

$$\begin{bmatrix} \mathbf{K}_{\mathrm{dd}} & \mathbf{0} & \mathbf{B}_{\mathrm{d}\lambda} & \mathbf{0} \\ \mathbf{0} & \mathbf{0} & \mathbf{R}_{\alpha\lambda} & \mathbf{0} \\ \mathbf{B}_{\lambda\mathrm{d}} & \mathbf{R}_{\lambda\alpha} & \mathbf{0} & -\mathbf{C}_{\lambda u} \\ \mathbf{0} & \mathbf{0} & -\mathbf{C}_{u\lambda} & \mathbf{0} \end{bmatrix} \begin{bmatrix} \mathbf{d} \\ \boldsymbol{\alpha} \\ \boldsymbol{\lambda}_{\mathrm{l}} \\ \mathbf{u}_{\mathrm{b}} \end{bmatrix} + \begin{bmatrix} \mathbf{M}_{\mathrm{dd}} & \mathbf{0} & \mathbf{0} & \mathbf{0} \\ \mathbf{0} & \mathbf{M}_{\alpha\alpha} & \mathbf{0} & \mathbf{0} \\ \mathbf{0} & \mathbf{0} & \mathbf{0} & \mathbf{0} \\ \mathbf{0} & \mathbf{0} & \mathbf{0} & \mathbf{0} \end{bmatrix} \begin{bmatrix} \ddot{\mathbf{d}} \\ \ddot{\boldsymbol{\alpha}} \\ \ddot{\boldsymbol{\lambda}}_{\mathrm{l}} \\ \ddot{\mathbf{u}}_{\mathrm{b}} \end{bmatrix} = \begin{bmatrix} \mathbf{f}_{\mathrm{d}} \\ \mathbf{f}_{\alpha} \\ \mathbf{0} \\ \mathbf{0} \end{bmatrix} \tag{44}$$

where $\mathbf{C}_{\lambda u} = \sum_m \mathbf{C}^m_{\lambda u}\,\mathbf{B}^m_{\mathrm{b}} = \mathbf{C}^{\mathrm{T}}_{u\lambda}$. In the static case the term involving accelerations drops out.

 

### 5.2. Forming stiffness and mass from existing FEM libraries

The foregoing matrix equations involve $\mathbf{K}^m_{\mathrm{dd}}$, $\mathbf{M}^m_{\mathrm{dd}}$ and $\mathbf{M}^m_{\alpha\alpha}$. These are the deformation-basis stiffness, deformation-basis mass and rigid-body motion mass matrices, respectively, for an individual subdomain. In practice these can be obtained from a standard finite element library as follows:

1. Using the available library, form the stiffness matrix $\mathbf{K}^m$ and mass matrix $\mathbf{M}^m$ for the subdomain $m$ by standard assembly techniques.
2. Extract a rigid-body mode basis $\boldsymbol{\Phi}^m_{\alpha}$ and a deformational basis $\boldsymbol{\Phi}^m_{\mathrm{d}}$ from the null and range space, respectively, of $\mathbf{K}^m$.
3. Orthonormalize so that $\boldsymbol{\Phi}^m_{\mathrm{d}}$ and $\boldsymbol{\Phi}^m_{\alpha}$ are biorthogonal with respect to $\mathbf{M}^m$. Take $\mathbf{R}^m = \boldsymbol{\Phi}^m_{\alpha}$.
4. Set $\mathbf{K}^m_{\mathrm{dd}} = (\boldsymbol{\Phi}^m_{\mathrm{d}})^{\mathrm{T}}\mathbf{K}^m\boldsymbol{\Phi}^m_{\mathrm{d}}$, $\mathbf{M}^m_{\mathrm{dd}} = (\boldsymbol{\Phi}^m_{d})^{\mathrm{T}}\mathbf{M}^m\boldsymbol{\Phi}^m_{\mathrm{d}}$, $\mathbf{M}^m_{\alpha\alpha} = (\mathbf{R}^m)^{\mathrm{T}}\mathbf{M}^m\mathbf{R}^m$.

For the static case one simply takes $\mathbf{K}^m_{\mathrm{dd}} = \mathbf{K}^m$, making maximum use of existing FEM libraries. It is necessary to extract the rigid-body basis $\mathbf{R}^m$, although this is not required to satisfy the mass orthogonality condition. In the dynamic case the procedure is more delicate; there is no explicit need, however, to explicitly compute the deformation modes $\boldsymbol{\Phi}^m_{\mathrm{d}}$ as shown by Park *et al.* [32].

### 5.3. Specializations

Equations (44) are valid for matching as well as non-matching meshes. For matched meshes with node-force-collocated multipliers, $\mathbf{B}_{\mathrm{d}\lambda}$, $\mathbf{R}_{\alpha\lambda}$ and $\mathbf{C}_{u\lambda}$ reduce to $\mathbf{B}_{\mathrm{b}}, \mathbf{R}_{\mathrm{b}} = \mathbf{B}^{\mathrm{T}}_{\mathrm{b}}\mathbf{R}$ and $\mathbf{C}_{\mathrm{b}} = \mathbf{B}^{\mathrm{T}}_{\mathrm{b}}\mathbf{L}$, respectively. Here $\mathbf{B}^{\mathrm{T}}_{\mathrm{b}}$ is a Boolean localization matrix that localizes the interface degrees of freedom, and $\mathbf{L}$ is the global assembly matrix such that $\mathbf{K}_{\mathrm{g}} = \mathbf{L}^{\mathrm{T}}\mathbf{K}\mathbf{L}$ is the global stiffness matrix of the non-partitioned structure. This is the equation used in the development of a simple dynamic parallel algorithm [32].

For static problems the inertial terms are dropped and $\mathbf{K}_{\mathrm{dd}}$ may be kept as $\mathbf{K}$ (the block diagonal supermatrix of all $\mathbf{K}^m$), giving

$$\begin{bmatrix} \mathbf{K} & \mathbf{0} & \mathbf{B}_{\mathrm{b}} & \mathbf{0} \\ \mathbf{0} & \mathbf{0} & \mathbf{R}^{\mathrm{T}}_{\mathrm{b}} & \mathbf{0} \\ \mathbf{B}^{\mathrm{T}}_{\mathrm{b}} & \mathbf{R}_{\mathrm{b}} & \mathbf{0} & -\mathbf{C}_{\mathrm{b}} \\ \mathbf{0} & \mathbf{0} & -\mathbf{C}^{\mathrm{T}}_{\mathrm{b}} & \mathbf{0} \end{bmatrix} \begin{bmatrix} \mathbf{d} \\ \boldsymbol{\alpha} \\ \boldsymbol{\lambda}_{\mathrm{l}} \\ \mathbf{u}_{\mathrm{b}} \end{bmatrix} = \begin{bmatrix} \mathbf{f}_{\mathrm{d}} \\ \mathbf{f}_{\alpha} \\ \mathbf{0} \\ \mathbf{0} \end{bmatrix} \tag{45}$$

The nodal deformation vector $\mathbf{d}$ can be obtained from the first matrix equation as $\mathbf{d} = \mathbf{F}(\mathbf{f}_{\mathrm{d}} - \mathbf{B}_{\mathrm{b}}\boldsymbol{\lambda}_{\mathrm{l}})$, where $\mathbf{F} = \mathbf{K}^{+}$ is the free–free flexibility, or Moore–Penrose generalized inverse of $\mathbf{K}$. This matrix can be efficiently obtained, subdomain by subdomain, as described in [33]. Substituting this into the third row gives $\mathbf{B}^{\mathrm{T}}_{\mathrm{b}}\mathbf{F}\,\mathbf{B}_{\mathrm{b}}\,\boldsymbol{\lambda}_{\mathrm{l}} - \mathbf{R}_{\mathrm{b}}\,\boldsymbol{\alpha} + \mathbf{C}_{\mathrm{b}}\,\mathbf{u}_{\mathrm{b}} = \mathbf{B}^{\mathrm{T}}_{\mathrm{b}}\,\mathbf{F}\,\mathbf{f}_{\mathrm{d}}$. Combining the second and fourth rows with that equation, one arrives at the following partitioned flexibility equation:

$$\begin{bmatrix} \mathbf{F}_{\mathrm{b}} & -\mathbf{R}_{\mathrm{b}} & -\mathbf{C}_{\mathrm{b}} \\ -\mathbf{R}^{\mathrm{T}}_{\mathrm{b}} & \mathbf{0} & \mathbf{0} \\ -\mathbf{C}^{\mathrm{T}}_{\mathrm{b}} & \mathbf{0} & \mathbf{0} \end{bmatrix} \begin{bmatrix} \boldsymbol{\lambda}_{\mathrm{l}} \\ \boldsymbol{\alpha} \\ \mathbf{u}_{\mathrm{b}} \end{bmatrix} = \begin{bmatrix} \mathbf{h}_{\mathrm{b}} \\ \mathbf{f}_{\alpha} \\ \mathbf{0} \end{bmatrix} \tag{46}$$

 

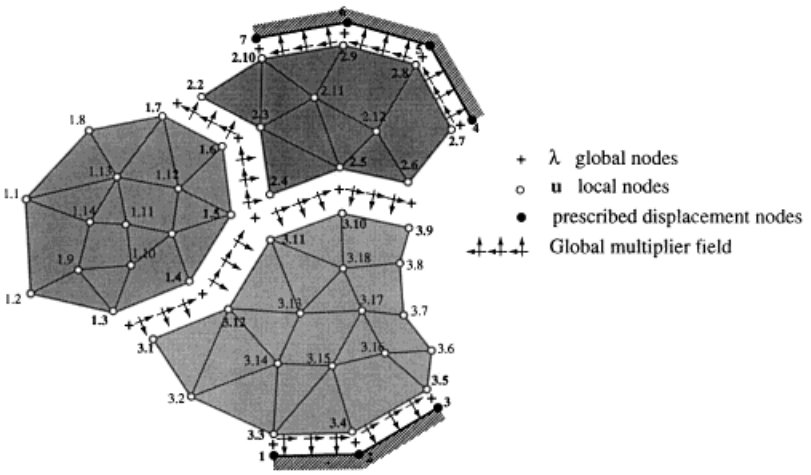


Figure 6. Matching-mesh, global-multiplier FEM discretization of example domain of Figure 1(c). Three node types are identified by indicated symbols. Prescribed displacement portions of the boundary are treated as internal interfaces

where $\mathbf{F}_b = \mathbf{B}_b^T \mathbf{F} \mathbf{B}_b$ and $\mathbf{h}_b = \mathbf{B}_b^T \mathbf{F} \mathbf{f}_d$. The latter has dimensions of displacement. Equation (46) links only the interface degrees of freedom.

The partitioned flexibility equation (46) and its dynamic counterpart have been applied to parallel computations by Park *et al.* [34, 35] to damage detection by Park *et al.* [36] to joint identification by Park and Felippa [37], and to distributed vibration control problems by Park and Kim [38].

### *5.4. Global multiplier FEM discretization*

Figure 6 shows a matched-mesh, FEM discretization of the example domain using global multipliers. The governing equations can be derived, for example, from the $\Pi_{\mathrm{PEM1}}$ functional. The details will not be worked out here, as they essentially lead to the equations summarized in Section 6.4.

It should be remarked that nodes with prescribed displacements can be treated in two ways. The one shown in Figure 6 carries additional multiplier and displacement unknowns. It leads, however, to a more modular implementation of the floating subdomain problem since all subdomains can be treated as free–free, while support boundary conditions are applied by the interface solver. In addition, the multipliers give directly the reactions, which are often of interest. Alternatively, the displacement conditions could be applied directly on the subdomain nodes, and the multipliers on $\partial\Omega_u$ dispensed with.

## 6. RELATED PRIOR WORK

This section summarizes specific publications or lines of research that have directly or indirectly influenced the work presented here. The notational scheme used by other authors has been modified as necessary to agree with our nomenclature.

 

### 6.1. The classical force method

Suppose the subdomains depicted in Figure 6 are an assembly of substructures connected by force-collocated global Lagrange multipliers arrayed in $\boldsymbol{\lambda}_b$. These are taken as the redundant forces of the classical force method. The governing matrix equations for this method [1, 39] may be compactly presented in the supermatrix form

$$\begin{bmatrix} \mathbf{F} & -\mathbf{I} & \mathbf{0} \\ -\mathbf{I} & \mathbf{0} & \mathbf{B}_1 \\ \mathbf{0} & \mathbf{B}_1^{\mathrm{T}} & \mathbf{0} \end{bmatrix} \begin{bmatrix} \mathbf{p} \\ \mathbf{v} \\ \boldsymbol{\lambda}_b \end{bmatrix} = \begin{bmatrix} \mathbf{0} \\ -\mathbf{B}_0 \mathbf{f}_b \\ \mathbf{0} \end{bmatrix} \tag{47}$$

Once this equation is solved, the interface displacement $\mathbf{u}_b$ can be recovered from

$$\mathbf{u}_b = \mathbf{B}_0^{\mathrm{T}} \mathbf{v} = \mathbf{F}_b \mathbf{f}_b \tag{48}$$

in which $\mathbf{F}_b = \mathbf{D}_{00} - \mathbf{D}_{10}^{\mathrm{T}} \mathbf{D}_{11}^{-1} \mathbf{D}_{10} = \mathbf{K}_b^{-1}$, $\mathbf{D}_{11} = \mathbf{B}_1^{\mathrm{T}} \mathbf{F} \mathbf{B}_1$ and $\mathbf{D}_{10} = \mathbf{B}_1^{\mathrm{T}} \mathbf{F} \mathbf{B}_0$.

In these equations $\mathbf{f}_b, \mathbf{p}$ and $\boldsymbol{\lambda}_b$ are vectors of applied, internal and redundant forces, respectively; $\mathbf{u}_b$ and $\mathbf{v}$ are the vectors of node displacements and internal deformations work-conjugate to $\mathbf{f}_b$ and $\mathbf{p}$, respectively; $\mathbf{B}_0$ and $\mathbf{B}_1$ are matrices that decompose the internal forces into statically determinate and indeterminate components, respectively; finally, $\mathbf{F}$ denotes the block-diagonal deformational flexibility matrix $\mathbf{diag}\{\mathbf{F}^m\}$, in which $\mathbf{F}^m$ is the deformational-flexibility matrix of the $m$th substructure. Both the deformation flexibility $\mathbf{F}$ and the so-called indeterminate flexibility $\mathbf{D}_{11}$ are required to be non-singular. If the structure is statically determinate, $\mathbf{B}_1$ and $\boldsymbol{\lambda}_b$ are void, and internal forces $\mathbf{p}$ can be determined directly from statics.

The challenge for implementing this method is the effective selection of the indeterminate force transmission matrix $\mathbf{B}_1$. Once this is done, $\mathbf{B}_0$ can be easily formed and all other quantities thereby obtained. Hence, most papers on the classical force method have focused on the algorithmic construction of $\mathbf{B}_1$ through clever choices of redundant force patterns. See, for instance, the surveys by Kaveh [40] and Felippa [41, 42]. Because $\mathbf{D}_{11}$ is full or quite dense, however, this method has not been competitive against the direct stiffness method version of the displacement method, particularly for the continuum FEM models that became popular in the 1960s. These points are further elaborated by Felippa and Park [43].

Comparing the classical force method (47) and (48) with the partitioned flexibility equations (45) and (46), we find that nothing in the latter requires user decisions or elaborated analysis of redundants. Once the meshes and partitions are set up, and rigid body mode bases obtained, matrices $\mathbf{B}, \mathbf{R}_b$ and $\mathbf{C}_b$ follow, and hence the construction of the patitioned flexibility equation (45) is automatic. The efficient solution of (45) is discussed by Park *et al.* [34, 35] and that of its dynamic counterpart by Park *et al.* [32].

In passing, we mention that Professor Gallagher had been pursuing the development of a 'modernized' force method for structural shape and topology optimization [44]. At this writing, the potential of the present partitioned flexibility equations (45) or its variants for use in such applications remains unexplored.

### 6.2. Fraeijs de Veubeke (1973)

A particularly relevant work is that presented by Fraeijs de Veubeke in a workshop lecture on matrix structural analysis delivered at the University of Calgary in 1973 [22]. The material examines in great detail intrinsic and connection properties of a discretized structure divided into

 

Table I. Comparisons of De Veubeke, Althuri, Farhat/Roux, and present formulations

| | De Veubeke (1973) | Atluri (1975) | Farhat and Roux (1994) | Present and Park and Felippa [37] |
|---|---|---|---|---|
| Formulation basis | Matrix methods of structural analysis | Continuum variational formulation | Equilibrium with constraints | Continuum variational formulation |
| Lagrangian multiplier | Global and generalized forces | Local and weighted average forces | Global and generalized forces | Local and physical point forces |
| Flexibility matrix | $\mathbf{F}$ (no detail) | Not derived | $\mathbf{F}=\mathbf{C}_\lambda^{\mathrm{T}}\mathbf{K}^{+}\mathbf{C}_\lambda$ | $\mathbf{F}_\mathrm{b}=\mathbf{B}_\mathrm{b}^{\mathrm{T}}\mathbf{K}^{+}\mathbf{B}_\mathrm{b}$ |
| Floating partition equilibrium | $\mathbf{R}^{\mathrm{T}}(\mathbf{f}+\mathbf{f}_\mathrm{b})=\mathbf{0}$ | Not considered | $\mathbf{R}^{\mathrm{T}}(\mathbf{f}+\mathbf{C}_\lambda\boldsymbol{\lambda}_\mathrm{b})=\mathbf{0}$ | $\mathbf{R}^{\mathrm{T}}\mathbf{B}_\mathrm{b}\boldsymbol{\lambda}_\mathrm{l}+\mathbf{f}_\alpha=\mathbf{0}$ |
| Interface constraints | $\mathbf{u}^{+}-\mathbf{u}^{-}=\mathbf{0}$ | $\mathbf{B}_\mathrm{b}u-\mathbf{C}_\mathrm{b}\mathbf{u}_\mathrm{b}=\mathbf{0}$ | $\mathbf{C}_\lambda^{\mathrm{T}}\mathbf{u}=\mathbf{0}$ | $\mathbf{B}_\mathrm{b}^{\mathrm{T}}\mathbf{d}+\mathbf{R}_\mathrm{b}\alpha$ $-\mathbf{C}_\mathrm{b}\mathbf{u}_\mathrm{b}=\mathbf{0}$ |
| Newton's third law | $\mathbf{t}^{+}+\mathbf{t}^{-}=0$ | $\mathbf{C}_{u\lambda}\boldsymbol{\lambda}_\mathrm{l}=\mathbf{0}$ | implicit in interface treatment | $\mathbf{C}_\mathrm{b}^{\mathrm{T}}\boldsymbol{\lambda}_\mathrm{l}=\mathbf{0}$ |

arbitrary elements, with no *a priori* preconceptions on element types. He spelled out the following matrix relations (italics below denote Fraeijs de Veubeke's terminology):

(a) *Transition conditions* between face + and face − of each interface:

$$\begin{aligned}\text{Displacements}: &\quad \mathbf{u}^{+}-\mathbf{u}^{-}=\mathbf{0}\\ \text{Tractions}: &\quad \mathbf{t}^{+}+\mathbf{t}^{-}=\mathbf{0}\end{aligned} \tag{49}$$

(b) *Statics at element level*:

$$\mathbf{R}^{\mathrm{T}}(\mathbf{f}+\mathbf{f}_\mathrm{b})=\mathbf{0} \tag{50}$$

where (in our notation) $\mathbf{R}$ is a basis for the element rigid-body modes, and $\mathbf{f}_\mathrm{b}$ and $\mathbf{f}$ are force vectors produced by boundary loads and body forces, respectively.

(c) *Generalized boundary displacement vector*:

$$\mathbf{u}_\mathrm{b}=\mathbf{F}(\mathbf{f}+\mathbf{f}_\mathrm{b})+\mathbf{R}\boldsymbol{\alpha} \tag{51}$$

where $\mathbf{F}$ is the deformational flexibility matrix and $\boldsymbol{\alpha}$ are rigid-body amplitudes.

These key relations, also summarized in Table I, provide the necessary tools to extend flexibility-based methods beyond the classical force method, which by then had already hit a dead end [42]. Unfortunately, the lecture did not provide the all-important implementation details. Furthermore the Notes were of limited dissemination, having only appeared in the 1980 Memorial Volume of selected papers.

 

### 6.3. *Atluri* (*1975*)

In the previously cited 1975 paper, Atluri [6] presented a systematic construction of hybrid elasticity functionals for finite element development work. The approach is to combine

$$\text{Hybrid functional} = \text{Canonical internal functional} + \text{Interface potential} \tag{52}$$

From the canonical functionals of linear elasticity, Atluri selected the Hu–Washizu, Hellinger–Reissner, potential energy (displacement) and complementary energy (equilibrium) forms. Two interface potential forms, herein called $\pi_u$ and $\pi_\lambda$, were considered. Of the various combinations studied by Atluri, those identified as HWM2 and HD2 are particularly relevant to the formulation of Section 3.

### 6.4. *Farhat and Roux* (*1991, 1994*)

The work of Farhat and Roux [23, 24] develops a practical implementation of flexibility methods driven by a specific objective: the efficient solution of FEM structural equations on massively parallel computers. Their derivations are summarized in Table I. The starting point is the constrained FEM stiffness equilibrium equations for a structure divided into matched subdomains

$$\begin{bmatrix} \mathbf{K} & \mathbf{C}_\lambda \\ \mathbf{C}_\lambda^{\mathrm{T}} & 0 \end{bmatrix} \begin{bmatrix} \mathbf{u} \\ \boldsymbol{\lambda}_{\mathrm{b}} \end{bmatrix} = \begin{bmatrix} \mathbf{f} \\ \mathbf{0} \end{bmatrix} \tag{53}$$

Here $\mathbf{K}$ is the partitioned block-diagonal partitioned stiffness matrix, $\mathbf{C}_\lambda$ the constraint matrix that enforces the interdomain continuity condition $\mathbf{u}^+ = \mathbf{u}^-, \mathbf{u}$ is the interior node displacement vector $\mathbf{f}$, the applied node force vector, and $\boldsymbol{\lambda}_{\mathrm{b}}$ is the vector of node-force-collocated Lagrange multipliers. Solving for $\mathbf{u}$ from the first row of (53) one gets

$$\mathbf{u} = \mathbf{K}^+(\mathbf{f} - \mathbf{C}_\lambda \boldsymbol{\lambda}_{\mathrm{b}}) + \mathbf{R}\boldsymbol{\alpha} \tag{54}$$

Here $\mathbf{K}^+$ is a generalized inverse of $\mathbf{K}$, $\mathbf{R}$ is a null-space basis of $\mathbf{K}$ whenever $\mathbf{K}$ is rank-deficient because of unsuppressed rigid body modes, and $\boldsymbol{\alpha}$ collects those modal amplitudes. Substituting (54) into the second row of (53) yields

$$\mathbf{C}_\lambda^{\mathrm{T}}[\mathbf{K}^+(\mathbf{f} - \mathbf{C}_\lambda \boldsymbol{\lambda}_{\mathrm{b}}) + \mathbf{R}\boldsymbol{\alpha}] = \mathbf{0} \tag{55}$$

Grouping (55) with the self-equilibrium equation (50) applied at the subdomain level, in which $\mathbf{f}_{\mathrm{b}} = -\mathbf{C}_\lambda \boldsymbol{\lambda}_{\mathrm{b}}$, one arrives at

$$\begin{bmatrix} \mathbf{C}_\lambda^{\mathrm{T}} \mathbf{K}^+ \mathbf{C}_\lambda & -\mathbf{C}_\lambda^{\mathrm{T}} \mathbf{R} \\ -\mathbf{R}^{\mathrm{T}} \mathbf{C}_\lambda & \mathbf{0} \end{bmatrix} \begin{bmatrix} \boldsymbol{\lambda}_{\mathrm{b}} \\ \boldsymbol{\alpha} \end{bmatrix} = \begin{bmatrix} \mathbf{C}_\lambda^{\mathrm{T}} \mathbf{K}^+ \mathbf{f} \\ -\mathbf{R}^{\mathrm{T}} \mathbf{f} \end{bmatrix} \tag{56}$$

which contains only interface variables. Equation (56) is solved iteratively by projected conjugate-gradient methods. Upon convergence the interior subdomain states are recovered from (54). Farhat and coworkers have developed projection operators that offer parallel scalability for structural problems, not only for three-dimensional solid elasticity problems but for plates and shells as well [25, 26]. These parallel structural algorithms, collectively identified as FETI (Finite Element Tearing and Interconnecting), represent one of the major advances in computational structural mechanics over the past decade.

 

### 6.5. *Interface potentials accounting for jump conditions*

In a recent survey of parametrized variational principles, one of the authors presented [45] a two-parameter, four-field form interface potential form that can be reduced to specific instances by adjusting the parameters. The varied local fields are the interface displacements $u_i$ and the boundary tractions $\sigma_{ni} = \sigma_{ij} n_j$ coming from the FEM mesh. The varied interface fields are the tractions $t_i$ and the partition frame displacements $u_{\mathrm{b}i}$. The two faces are labeled $-$ and $+$. A generalization over the potentials considered previously is the allowance of displacement and traction jumps at any point of the interface:

$$[\![u_i]\!] = u_i^+ - u_i^-, \quad [\![t_i]\!] = \sigma_{ni}^+ + \sigma_{ni}^- \quad \text{on } \partial\Omega_{\mathrm{b}} \tag{57}$$

If the 'transition conditions' (49) are verified both jumps vanish. Prescribed jumps are resolved by setting

$$u_i^+ = u_{\mathrm{b}i} + \tfrac{1}{2}[\![u_i]\!], \quad u_i^- = u_{\mathrm{b}i} - \tfrac{1}{2}[\![u_i]\!], \quad \sigma_{ni}^+ = t_i + \tfrac{1}{2}[\![t_i]\!], \quad \sigma_{ni}^- = -t_i + \tfrac{1}{2}[\![t_i]\!] \tag{58}$$

where $u_{\mathrm{b}i} = (u_i^+ + u_i^-)/2$ and $t_i = (\sigma_{ni}^+ - \sigma_{ni}^-)/2$. The parametrized interface functional that treats all of the above as weak constraints is

$$\begin{aligned}\pi(u_i, \sigma_{ni}, u_{\mathrm{b}i}, t_i) = \int_{\partial\Omega_{\mathrm{b}}} & [(2(\alpha_1 - \alpha_2)t_i + \alpha_2(\sigma_{ni}^+ - \sigma_{ni}^-))(u_i^+ - u_i^- - [\![u_i]\!]) + \alpha_1 [\![t_i]\!](u_i^+ + u_i^-) \\ & + (1 - 2\alpha_1)(\sigma_{ni}^+(u_i^+ - u_{\mathrm{b}i} - \tfrac{1}{2}[\![u_i]\!]) + \sigma_{ni}^-(u_i^- - u_{\mathrm{b}i} + \tfrac{1}{2}[\![d_i]\!]) + u_{\mathrm{b}i}[\![t_i]\!])]\,\mathrm{d}S\end{aligned} \tag{59}$$

Here $\alpha_1$ and $\alpha_2$ are free parameters. This generalizes a form proposed by Fraeijs de Veubeke in 1974 [15]. The special case in which $\alpha_1 = \frac{1}{2}$, $\alpha_2 = 0$, $[\![u_i]\!] = 0$ and $[\![t_i]\!] = 0$ results in

$$\pi(u_i, t_i) = \int_{\partial\Omega_{\mathrm{b}}} t_i(u_i^+ - u_i^-)\,\mathrm{d}S \tag{60}$$

which with the notational change $t_i \to \lambda_{\mathrm{b}i}$ becomes the $\pi_\lambda$ of the method of global Lagrange multipliers introduced in Section 3.5. Setting $\alpha_1 = \alpha_2 = 0$ together with $[\![u_i]\!] = 0$ and $[\![t_i]\!] = 0$ results in

$$\pi(u_i, \sigma_{ni}, u_{\mathrm{b}i}) = \int_{\partial\Omega_{\mathrm{b}}} [\sigma_{ni}^+(u_i^+ - u_{\mathrm{b}i}) + \sigma_{ni}^-(u_i^- - u_{\mathrm{b}i})]\,\mathrm{d}S \tag{61}$$

which with the notational change $\sigma_{ni}^+ \to \lambda_{\mathrm{l}i}^+$ and $\sigma_{ni}^- \to \lambda_{\mathrm{l}i}^-$ becomes the $\pi_u$ of the method of localized Lagrange multipliers introduced in Section 3.2.

While an actual displacement jump is uncommon (aside from contact, impact and crack propagation problems), traction jumps can occur on physical interfaces, such as joints, subject to interface loads or wave propagation. This extension of partitioned analysis is under investigation.

## 7. SUMMARY AND CONCLUSIONS

We have presented a continuum-based variational formulation for the partitioned analysis of linear structural systems. The varied fields are the deformational and rigid-body displacements of each

 

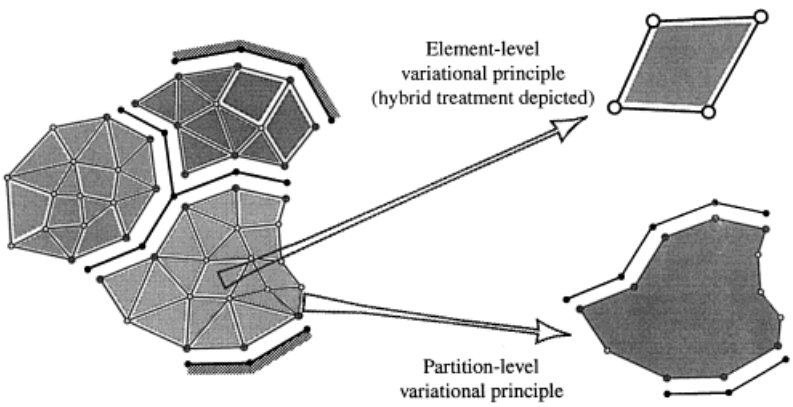


Figure 7. Multilevel/hierarchical use of variational principles. The variational principle(s) used for development of individual elements may be different from that used for partitions that groups such elements. This strategy is generally inevitable if a partition contain different element types

partition, the global displacements of partition frames, and localized Lagrange multipliers that enforce interface displacement compatibility.

The most important ingredients of the variational formulation are: the use of localized Lagrange multiplier fields, and the decomposition of the substructural displacements into deformational and rigid body. The latter is instrumental in providing separate equilibrium equations for each partition viewed as a rigid body and as a flexible body. This separation is important in implementing accurate dynamic time-stepping solvers as well as handling floating subdomains. The multiplier localization simplifies the treatment of non-matching mesh interfaces, as well as that of cross points in matched interfaces.

The discrete equations were obtained using the potential energy canonical functional for the internal fields. This was done for expediency since the paper focuses on the treatment of the interfaces. Nothing prohibits the use of internal functionals with independently varied stress and/or strain fields, such as the Hu–Washizu or Hellinger–Reissner principles or, more generally, parametrized variational forms [11, 45].

In practice, however, the application of variational principles to partitioned analysis is best viewed in a *multilevel/hierarchical* framework. This is illustrated in Figure 7. The variational principle(s) used to develop individual elements need not be the same as that used to link up the partitions, as long as they produce elements with the standard displacement degrees of freedom. In fact the key ingredient for the partition-level principle is the interface potential rather than the interior functional. Two advantages of this approach should be noted:

(a) If partitions combine distinct elements types, it is likely that they come from different variational formulations. Hence a multilevel strategy is inevitable.
(b) It simplifies the use of element matrices from existing FEM libraries. In the case of models assembled from commercial software, the element formulation basis is often unknown. Coupling techniques that do not require such information are obviously preferable from the standpoint of modularity. As noted in the Introduction, partitioned analysis should ideally focus on modelling the interaction separately from the components.

 

The question of how to select interface interpolation functions to maintain rank sufficiency and consistency (the latter being verifiable by interface patch tests) remains a topic of current research.

Two related topics are addressed in separate papers. If the deformational displacement field is transformed into strains, the resulting equations have been found attractive for system identification, damage detection and localized vibration control, which collectively form a set of important inverse problems. These topics have been covered by Park *et al.* [36], Park and Kim [38] and Park and Reich [46, 47]. An extension of the present variational principle to interaction of flexible structures with an internal acoustic fluid has been developed by Park *et al.* [48].

ACKNOWLEDGEMENTS

The present work has been supported by the National Science Foundation under the grant High Performance Computer Simulation of Multiphysics Problems (award ECS-9725504) and by Sandia National Laboratories under the Accelerated Strategic Computational Initiative (ASCI) contracts AS-5666 and AS-9991.

REFERENCES

1. Argyris JH, Kelsey S. *Energy Theorems and Structural Analysis*. Butterworths: London, 1960: reprinted from *Aircraft Engineering* **26**, Oct–Nov 1954 and **27**, April–May 1955.
2. Fraeijs de Veubeke BM. Displacement and equilibrium models. In *Stress Analysis*, Zienkiewicz OC, Hollister G. (eds). Wiley: London, 1965; 145–197.
3. Washizu K. *Variational Methods in Elasticity and Plasticity*. Pergamon Press: New York, 1968.
4. Pian THH, Tong P. Basis of finite element methods for solid continua. *International Journal for Numerical Methods in Engineering* 1969; **1**:3–29.
5. Pian THH. Finite element methods by variational principles with relaxed continuity requirements. In *Variational Methods in Engineering*, vol. 1, Brebbia CA, Tottenham H. (eds). Southampton University Press: Southampton, U.K., 1973.
6. Atluri SN. On 'hybrid' finite-element models in solid mechanics. In *Advances in Computer Methods for Partial Differential Equations*, Vichnevetsky R (ed.). AICA: Rutgers University, 1975; 346–356.
7. Oden JT, Reddy JN. *Variational Methods in Theoretical Mechanics*. Springer: Berlin, 1982.
8. Reddy JN. *Energy and Variational Methods in Applied Mechanics*. Wiley/Interscience: New York, 1984.
9. Hughes TJR. *The Finite Element Method: Linear Static and Dynamic Finite Element Analysis*. Prentice-Hall: Englewood Cliffs, NJ, 1987.
10. Zienkiewicz OC, Taylor RE. *The Finite Element Method* (4th edn), vol I. McGraw-Hill: New York; 1989.
11. Felippa CA. A survey of parameterized variational principles and applications to computational mechanics. *Computer Methods in Applied Mechanics and Engineering* 1994; **113**:109–139.
12. Pian THH. Derivation of element stiffness matrices by assumed stress distributions. *AIAA Journal* 1964; **2**: 1333–1336.
13. Herrmann LR. A bending analysis for plates, In *Proceedings 1st Conference on Matrix Methods in Structural Mechanics*, AFFDL-TR-66-80, Air Force Institute of Technology, Dayton, Ohio, 1966; 577–604.
14. Fraeijs de Veubeke BM. A new variational principle for finite elastic displacements. *International Journal of Engineering Science* 1972; **10**:745–763, .
15. Fraeijs de Veubeke BM. Variational principles and the patch test. *International Jounral for Numerical Methods in Engineering* 1974; **8**:783–801.
16. Courant R, Hilbert D. *Methods of Mathematical Physics*. vol I. Interscience: New York, 1953.
17. Sewell MJ. *Maximum and Minimum Principles*. Cambridge: England, 1987.
18. Lagrange J-L. *Mécanique Analytique*. 1788 (1965 edn. complète), 2 vols. Blanchard: Paris, 1965.
19. Lanczos C. *The Variational Principles of Mechanics* (4th edn.), Dover: New York, 1970.
20. Dugas R. *A History of Mechanics*. Dover: New York, 1988; 332–338.
21. Park KC, Felippa CA. A variational framework for solution method developments in structural mechanics. *Journal of Applied Mechanics* 1998; **65**(1):242–249.

 

22. Fraeijs de Veubeke BM. Matrix structural analysis: Lecture Notes for the International Research Seminar on the Theory and Application of Finite Element Methods. Calgary, Alberta, Canada, July–August 1973; reprinted in *B.M. Fraeijs de Veubeke Memorial Volume of Selected Papers*, Geradin M (ed.). Sitthoff & Noordhoff, Alphen aan den Rijn: The Netherlands, 1980; 509–568.
23. Farhat C, Roux F-X. A method of finite element tearing and interconnecting and its parallel solution algorithm *International Journal for Numerical Methods in Engineering* 1991; **32**:1205–1227.
24. Farhat C, Roux F-X. Implicit parallel processing in structural mechanics. *Computational Mechanics Advances* 1994; **2**:1–124.
25. Farhat C, Mandel J. The two-level FETI method for static and dynamic plate problems—Part I: an optimal iterative solver for biharmonic systems. *Computer Methods in Applied Mechanics and Engineering* 1998; **155**:129–151.
26. Farhat C, Chen P-S, Mandel J, Roux F-X. The two-level FETI method for static and dynamic plate problems—Part II: Extension to shell problems, parallel implementation and performance results. *Computer Methods in Applied Mechanics and Engineering* 1998; **155**:153–179.
27. Prager W. Variational principles for linear elastostatics for discontinuous displacements, strains and stresses. In *Recent Progress in Applied Mechanics*, The Folke-Odgvist Vol. Broger B, Hult J, Niordson F (eds). Almqusit and Wiksell: Stockholm, 1967; 463–474.
28. Tong P. New displacement finite element method for solid continua. *International Journal for Numerical Methods in Engineering* 1970; **2**:73–83.
29. Bergan PG, Nygåard MK. Finite elements with increased freedom in choosing shape functions. *International Journal for Numerical Methods in Engineering* 1984; **20**:643–664.
30. Felippa CA. Parametrized multifield variational principles in elasticity: II. Hybrid functionals and the Free Formulation. *Communications in Applied Numerical Methods* 1989; **5**:89–98.
31. Bernardi C, Maday Y, Patera AT. A new nonconforming approach to domain decomposition: the mortar element method. *Technical Report*, Université Pierre at Marie Curie, Paris, France, January 1990.
32. Gumaste U, Park KC, Alvin KF. A family of implicit partitioned time integration algorithms for parallel analysis of heterogeneous structural systems. *Computational Mechanics*, to appear 1999.
33. Felippa CA, Park KC, Justino MR. The construction of free-free flexibility matrices as generalized stiffness inverses. *Computers and Structures* 1998; **68**:411–418.
34. Justino MR, Park KC, Felippa CA. An algebraically partitioned FETI method for parallel structural analysis: implementation and numerical performance evaluation. *International Journal for Numerical Methods in Engineering* 1997; **40**:2739–2758.
35. Park KC, Justino MR, Felippa CA. An algebraically partitioned FETI method for parallel structural analysis: algorithm description. *International Journal for Numerical Methods in Engineering* 1997; **40**:2717–2737.
36. Park KC, Reich GW, Alvin KF. Damage detection using localized flexibilities. In *Structural Health Monitoring, Current Status and Perspectives*, Chang F-K (ed.). Technomic Pub., 1997; 125–139.
37. Park KC, Felippa CA. A flexibility-based inverse algorithm for identification of structural joint properties. Proceedings of *ASME Symposium on Computational Methods on Inverse Problems*, Anaheim, CA, 15–20 November 1998.
38. Park KC, Kim N-I. A theory of localized vibration control via partitioned LQR synthesis. Center for Aerospace Structures, Report No. CU-CAS-98-13, University of Colorado, Boulder, CO, July 1998; also *Proceedings XXI Congresso Nacional de Matematica Applicada e Computacional*, Caxambu, MG, Brazil, September 1998.
39. Pestel EC, Leckie FA. *Matrix Methods in Elastomechanics*. McGraw-Hill: New York, 1963.
40. Kaveh A. Recent developments in the force method of structural analysis. *Applied Mechanics Reviews* 1992; **45**(9):401–418.
41. Felippa CA. Will the force method come back? Journal of Applied Mechanics 1987; **54**:728–729.
42. Felippa CA. Parametric unification of matrix structural analysis: classical formulation and d-connected mixed elements. *Finite Elements Analysis Design* 1995; **21**:45–74.
43. Felippa CA, Park KC. A direct flexibility method. *Computer Methods in Applied Mechanics and Engineering* 1997; **149**:319–337.
44. Gallagher RH. Private communication to Park KC, 1997.
45. Felippa CA. Recent developments in parametrized variational principles for mechanics. *Computational Mechanics* 1996; **18**:159–174.
46. Park KC, Reich GW. A theory for strain-based structural system identification. *Proceedings of 9th International Conference on Adaptive Structures and Technologies*, 14–16 October 1998, Cambridge, MA.
47. Park KC, Reich GW. A procedure to determine accurate rotations from measured strains and displacements for system identification. Center for Aerospace Structures, Report No. CU-CAS-98-16, University of Colorado, Boulder, CO, July 1998; *Proceedings of 17th International Modal Analysis Conference*, 8–11 February 1999, Kissimmee, FL.
48. Park KC, Felippa CA, Ohayon R. Partitioned formulation of internal fluid-structure interaction problems via localized Lagrange multipliers. Center for Aerospace Structures, Report No. CU-CAS-98-14, University of Colorado, Boulder, CO, July 1998; *Computer Methods in Applied Mechanics and Engineering*, 1999, to appear.

 